

OPTIMAL ESTIMATION OF GENERIC DYNAMICS BY PATH-DEPENDENT NEURAL JUMP ODES

Florian Krach¹ Marc Nübel Josef Teichmann¹

¹Department of Mathematics, ETH Zurich, Switzerland,
{firstname.lastname}@math.ethz.ch

ABSTRACT

This paper studies the problem of forecasting general stochastic processes using an extension of the Neural Jump ODE (NJ-ODE) framework (Herrera et al., 2021). While NJ-ODE was the first framework to establish convergence guarantees for the prediction of irregularly observed time-series, these results were limited to data stemming from Itô-diffusions with complete observations, in particular Markov processes where all coordinates are observed simultaneously. In this work, we generalise these results to generic, possibly non-Markovian or discontinuous, stochastic processes with incomplete observations, by utilising the reconstruction properties of the signature transform. These theoretical results are supported by empirical studies, where it is shown that the path-dependent NJ-ODE outperforms the original NJ-ODE framework in the case of non-Markovian data. Moreover, we show that PD-NJ-ODE can be applied successfully to limit order book (LOB) data.

1 INTRODUCTION

The processing and prediction of time series data is of great importance in many data-driven fields such as economics, finance and medicine. In recent years a lot of progress was made improving the machine learning techniques and, in particular, the neural network based ones, to be able to deal with more and more complicated problem settings. Recurrent Neural networks (RNNs) constituted the starting point to deal with discrete time series of variable and possibly unbounded length. Their main constraint is the underlying assumption that observations occur in regular time steps. A first step in the direction of irregular observation times was made by defining the RNN's latent variable continuously in time with some time-decay (e.g. exponential) directed to 0 (Che et al., 2018; Cao et al., 2018). However, since this is a rather stiff framework, neural ODEs (Chen et al., 2018) set a new milestone by making the continuously-in-time defined latent dynamics trainable through a neural network. Finally, combining this trainable continuous-in-time latent framework with an RNN cell, led to a framework for irregularly sampled time series data (Rubanova et al., 2019; Brouwer et al., 2019).

In machine learning applications to time series data, we distinguish between two different problem settings. Firstly, the labelling problem, where the entire time series is processed with the goal to determine a class or value describing some feature of this time series. An example would be a time series consisting of health parameters of a hospital patient with the aim of predicting whether the patient will develop a certain disease within the next days. And secondly, the forecasting problem where the goal is to process the known past values of the time series to predict how it will develop in the future. If this is done such that the entire time series of a predefined length is processed and certain time points in the future are predicted, then this can be viewed as a special case of the labelling problem (with a possibly infinite dimensional output). Here, we will refer to this as *offline forecasting*. On the other hand, if the goal is to forecast continuously in time, where for every time point a prediction can be made depending only on the past observations, this is a different problem, which we refer to as *online forecasting*. Here the algorithm has to dynamically predict based on the known past observations as long as no new information is available and then processes new observations (and adjust itself accordingly), whenever they become available. Coming back to our previous example, this would mean to continuously in time forecast how the health parameters will evolve, given those observations which were made up to the current time. In this work, which is the second part and generalisation of the Neural Jump ODE (NJ-ODE) framework (Herrera et al.,

2021), we consider precisely this problem. In particular, our goal is to make optimal forecasts, where optimality in this work is meant in terms of the L^2 -norm.

While NJ-ODE was the first framework in which theoretical convergence guarantees of the model output to the optimal prediction were derived, relatively restrictive assumptions on the underlying dynamics of the time series data were needed. In particular, the data has to stem from an Itô diffusion with several constraints on its drift and diffusion. This implies that paths of the dataset are continuous and Markovian (i.e. without path-dependence). Moreover, it is necessary that observations are complete, i.e., that all coordinates are observed simultaneously at each observation time. In the present work, we extend the NJ-ODE such that it can be applied to a very general set of stochastic processes that satisfy only weak regularity conditions. Since some of these constraints might seem a bit abstract at first, we provide several examples for which we prove that they satisfy them. Some examples are processes with jumps, fractional Brownian motion (i.e. rough paths with path dependence) and multidimensional correlated processes with incomplete observations. Moreover, we discuss that the independence between observation times and the underlying process is not needed and show, how the NJ-ODE framework can be used to perform not only prediction but also uncertainty estimation. The working horse for our theoretical results is, beside neural networks, the signature transform with its universal approximation property.

1.1 RELATED WORK

Recurrent neural networks (Rumelhart et al., 1985; Jordan, 1997) and the neural ODE (Chen et al., 2018) are the two main ingredients for the (path-dependent) NJ-ODE model. The first works in which they were combined to a model similar to the one we use were (Rubanova et al., 2019; Brouwer et al., 2019). In contrast to our framework, the latent ODE (Rubanova et al., 2019) is a model for the offline forecasting problem, where an encoder-decoder type model is used. First, the ODE-RNN encoder processes the entire time series of observations to generate an initial latent variable, which is then used as starting point for a neural ODE that produces the forecasts. In comparison to that, GRU-ODE-Bayes (Brouwer et al., 2019) uses the same model framework as we do for online forecasting. The main difference to NJ-ODE lies in the objective function and training framework. In particular, no convergence guarantees exist for GRU-ODE-Bayes, as was discussed in detail in (Herrera et al., 2021).

Being the predecessor, NJ-ODE (Herrera et al., 2021) clearly is the most related work to the present one. While the main structure of the model and of the theoretical results is the same, we make many important changes to extend the theory from a class of Itô processes to a large class of generic stochastic processes. A major ingredient to do this is the signature transform (Chevyrev & Kormilitzin, 2016; Kiraly & Oberhauser, 2019; Fermanian, 2020), which allows us to approximate path dependent behaviours.

The most related work in the context of the labelling problem, besides (Rubanova et al., 2019), is the neural controlled differential equation (NCDE) (Kidger et al., 2020). Similar to neural ODEs, it integrates a neural network, however, not against time but against the (spline) interpolation of the observed time series.

2 PROBLEM SETTING

We assume to have a time-series of observations of a continuous-time stochastic process, where the observation times and the observed coordinates are random. In the following we give precise definitions together with the needed assumptions to establish our theoretical guarantees, following the descriptions in (Herrera et al., 2021).

2.1 STOCHASTIC PROCESS, RANDOM OBSERVATION TIMES AND OBSERVATION MASK

Let $d_X \in \mathbb{N}$ and $T > 0$ be the fixed time horizon. Consider a filtered probability space $(\Omega, \mathcal{F}, \mathbb{F} := \{\mathcal{F}_t\}_{0 \leq t \leq T}, \mathbb{P})$, on which an adapted càdlàg stochastic process¹ $X := (X_t)_{t \in [0, T]}$ taking values in

¹A stochastic process is a collection of random variables $X_t : \Omega \rightarrow \mathbb{R}^{d_X}, \omega \mapsto X_t(\omega)$ for $0 \leq t \leq T$.

\mathbb{R}^{d_x} is defined. We define the running maximum process

$$X_t^* := \sup_{0 \leq s \leq t} |X_s|, \quad 0 \leq t \leq T.$$

Moreover, let \mathcal{J} be the random set of discontinuity times of X , defined for every $\omega \in \Omega$ as $\mathcal{J}(\omega) := \{t \in [0, T] \mid \Delta X_t(\omega) \neq 0\}$.

We consider another probability space $(\tilde{\Omega}, \tilde{\mathcal{F}}, \tilde{\mathbb{P}})$, on which the random observation times of the stochastic process are defined. In particular, we define

- $n : \tilde{\Omega} \rightarrow \mathbb{N}_{\geq 0}$, a random variable with $\mathbb{E}_{\tilde{\mathbb{P}}}[n] < \infty$, which is the random number of observations, and
- $t_i : \tilde{\Omega} \rightarrow [0, T]$ for $0 \leq i \leq n$, the *sorted*² random variables, describing the random observation times.

Moreover, we let $K := \max \left\{ k \in \mathbb{N} \mid \tilde{\mathbb{P}}(n \geq k) > 0 \right\} \in \mathbb{N} \cup \{\infty\}$ be the maximal value of n . We use the notation $\mathcal{B}([0, T])$ for the Borel σ -algebra of the set $[0, T]$ and define for each $1 \leq k \leq K$

$$\lambda_k : \mathcal{B}([0, T]) \rightarrow [0, 1], \quad B \mapsto \lambda_k(B) := \frac{\tilde{\mathbb{P}}(n \geq k, (t_k -) \in B)}{\tilde{\mathbb{P}}(n \geq k)},$$

which is a probability measure on the time interval $[0, T]$ as shown in (Herrera et al., 2021). The time of the last observation before a certain time t is defined as

$$\tau : [0, T] \times \tilde{\Omega} \rightarrow [0, T], \quad (t, \tilde{\omega}) \mapsto \tau(t, \tilde{\omega}) := \max\{t_i(\tilde{\omega}) \mid 0 \leq i \leq n(\tilde{\omega}), t_i(\tilde{\omega}) \leq t\}.$$

The observation mask $M = (M_k)_{0 \leq k \leq K}$ is a sequence of random variables on $(\tilde{\Omega}, \tilde{\mathcal{F}}, \tilde{\mathbb{P}})$ taking values in $\{0, 1\}^{d_x}$ such that the j -th coordinate of the k -th element of the sequence, i.e. $M_{k,j}$, signals whether the j -th coordinate of the stochastic process, denoted $X_{t_k,j}$, is observed at observation time t_k . In particular, $M_{k,j} = 1$ means that it is observed, while $M_{k,j} = 0$ means that it is not. By abuse of notation, we also write $M_{t_k} := M_k$.

2.2 INFORMATION σ -ALGEBRA

We define the σ -algebra, that describes which information is available at any time t . In the following, we leave away $\tilde{\omega} \in \tilde{\Omega}$ whenever the meaning is clear. We define the filtration of the currently available information $\mathbb{A} := (\mathcal{A}_t)_{t \in [0, T]}$ by

$$\mathcal{A}_t := \sigma(X_{t_i,j} \mid t_i \leq t, j \in \{1 \leq l \leq n \mid M_{t_i,l} = 1\}),$$

where t_i are the observation times and $\sigma(\cdot)$ denotes the generated σ -algebra. By the definition of τ we have $\mathcal{A}_t = \mathcal{A}_{\tau(t)}$ for all $t \in [0, T]$. $(\Omega \times \tilde{\Omega}, \mathcal{F} \otimes \tilde{\mathcal{F}}, \mathbb{F} \otimes \tilde{\mathcal{F}}, \mathbb{P} \times \tilde{\mathbb{P}})$ is the filtered product probability space which, intuitively speaking, combines the randomness of the stochastic process with the randomness of the observations. Here, $\mathbb{F} \otimes \tilde{\mathcal{F}}$ consists of the tensor-product σ -algebras $(\mathcal{F} \otimes \tilde{\mathcal{F}})_t := \mathcal{F}_t \otimes \tilde{\mathcal{F}}$ for $t \in [0, T]$. For more details we refer the interested reader to (Herrera et al., 2021).

2.3 NOTATION AND ASSUMPTIONS ON THE STOCHASTIC PROCESS X

We denote the conditional expectation process of X by $\hat{X} = (\hat{X}_t)_{0 \leq t \leq T}$, defined by $\hat{X}_t := \mathbb{E}_{\mathbb{P} \times \tilde{\mathbb{P}}}[X_t \mid \mathcal{A}_t]$ and remark that in contrast to the setting in (Herrera et al., 2021), $\hat{X}_{\tau(t)} \neq X_{\tau(t)}$ in general, since observations are incomplete. Moreover, we define for any $0 \leq t \leq T$ the process $\tilde{X}^{\leq t}$ to be the continuous version of the rectilinear interpolation of the observations of X until time t . Its j -th coordinate at time $0 \leq s \leq T$ is given by

$$\tilde{X}_{s,j}^{\leq t} := \begin{cases} X_{t_{\ell(s,t)},j} \frac{t_{\ell(s,t)} - s}{t_{\ell(s,t)} - t_{\ell(s,t)-1}} + X_{t_{\ell(s,t)-1},j} \frac{s - t_{\ell(s,t)-1}}{t_{\ell(s,t)} - t_{\ell(s,t)-1}}, & \text{if } t_{\ell(s,t)-1} < s \leq t_{\ell(s,t)}, \\ X_{t_{\ell(s,t)},j}, & \text{if } s \leq t_{\ell(s,t)-1}, \end{cases}$$

²For all $\tilde{\omega} \in \tilde{\Omega}$, $0 = t_0 < t_1(\tilde{\omega}) < \dots < t_n(\tilde{\omega})(\tilde{\omega}) \leq T$.

where

$$\begin{aligned} l(s, t) &:= l(s, t, j) := \max\{0 \leq l \leq n \mid t_l \leq \min(s, t), M_{t_l, j} = 1\}, \\ \ell(s, t) &:= \ell(s, t, j) := \inf\{1 \leq \ell \leq n \mid s \leq t_\ell \leq t, M_{t_\ell, j} = 1\}, \end{aligned}$$

with the standard definition that the infimum of the empty set is ∞ and the additional definition that $t_\infty := T$. In particular, $\tilde{X}^{\leq t}$ is the rectilinear interpolation (sometimes denoted as forward-fill), except that its jumps at $t_{l(s, t)}$ are replaced by linear interpolations between the previous observation time $t_{l(s, t)-1}$ and $t_{l(s, t)}$. It is important to note, that this is not solely a coordinate-wise interpolation, since the given coordinate might not have been observed at the previous observation time. Moreover, by this definition, $\tilde{X}^{\leq \tau(t)}$ is $\mathcal{A}_{\tau(t)}$ -measurable for all t , and for any $r \geq t$ and all $s \leq \tau(t)$ we have $\tilde{X}_s^{\leq \tau(t)} = \tilde{X}_s^{\leq \tau(r)}$.

Using $\mathcal{A}_t = \mathcal{A}_{\tau(t)}$ and that $\tilde{X}^{\leq \tau(t)} \in \mathcal{A}_{\tau(t)}$ carries all information available³ in $\mathcal{A}_{\tau(t)}$, we know by the Doob-Dynkin Lemma (Taraldsen, 2018, Lemma 2) that there exist measurable functions $F_j : [0, T] \times [0, T] \times BV^c([0, T]) \rightarrow \mathbb{R}$ such that $\hat{X}_{t, j} = F_j(t, \tau(t), \tilde{X}^{\leq \tau(t)})$. The following assumptions are central to establish our theoretical results. Examples where these assumptions are satisfied are given in Section 6.

Assumption 2.1. *We assume that*

1. *for every $1 \leq k, l \leq K$, M_k is independent of t_l and of n , $\tilde{\mathbb{P}}(M_{k, j} = 1) > 0$ and $M_{0, j} = 1$ for all $1 \leq j \leq d_X$ (i.e. every coordinate can be observed at any observation time and X is completely observed at 0) and $|M_k|_1 > 0$ for every $1 \leq k \leq K$ $\tilde{\mathbb{P}}$ -almost surely (i.e. at every observation time at least one coordinate is observed),*
2. *the probability that any two observation times are closer than $\epsilon > 0$ converges to 0 when ϵ does, i.e. if $\delta(\tilde{\omega}) := \min_{0 \leq i \leq n(\tilde{\omega})} |t_{i+1}(\tilde{\omega}) - t_i(\tilde{\omega})|$ then $\lim_{\epsilon \rightarrow 0} \tilde{\mathbb{P}}(\delta < \epsilon) = 0$,*
3. *almost surely X is not observed at a jump, i.e. $(\mathbb{P} \times \tilde{\mathbb{P}})(t_j \in \mathcal{J} \mid j \leq n) = (\mathbb{P} \times \tilde{\mathbb{P}})(\Delta X_{t_j} \neq 0 \mid j \leq n) = 0$ for all $1 \leq j \leq K$,*
4. *F_j are continuous and differentiable in their first coordinate t such that their partial derivatives with respect to t , denoted by f_j , are again continuous and there exists a $B > 0$ and $p \in \mathbb{N}$ such that for every $t \in [0, T]$ the functions f_j, F_j are polynomially bounded in X^* , i.e.*

$$|F_j(\tau(t), \tau(t), \tilde{X}^{\leq \tau(t)})| + |f_j(t, \tau(t), \tilde{X}^{\leq \tau(t)})| \leq B(X_t^* + 1)^p,$$
5. *X^* is L^{2p} -integrable, i.e. $\mathbb{E}[(X_T^*)^{2p}] < \infty$.*

Remark 2.2. *Assumption 2.1 2. is a technical condition that is needed to get compact subsets of $BV([0, T])$. It is for example satisfied, if the interarrival times between observations are i.i.d. exponential random variables.*

Under Assumption 2.1 we can rewrite \hat{X} by the fundamental theorem of calculus as

$$\hat{X}_{t, j} = F_j(\tau(t), \tau(t), \tilde{X}^{\leq \tau(t)}) + \int_{\tau(t)}^t f_j(s, \tau(t), \tilde{X}^{\leq \tau(t)}) ds,$$

implying that it is càdlàg. We remark that jumps of \hat{X} occur only at new observation times, i.e., at t_i , for $1 \leq i \leq n$.

2.4 OPTIMAL APPROXIMATION

As in (Herrera et al., 2021), we are interested in the L^2 -optimal approximation of X given the available information \mathcal{A} . The following result was proven in (Herrera et al., 2021, Proposition B.1) and shows that this approximation is given by the conditional expectation process \hat{X} .

³More precisely, this is only true if the probability of any consecutive observations being equal is zero. If this is not the case, one can add to $\tilde{X}^{\leq t}$ coordinates which describe the coordinate-wise amount of observations as paths that increases by 1, whenever a new observation is made for this coordinate. To get continuity of these paths, the same interpolation as for $\tilde{X}^{\leq t}$ can be used.

Proposition 2.3. *The optimal (i.e. L^2 -norm minimizing) process in $L^2(\Omega \times \tilde{\Omega}, \mathbb{A}, \mathbb{P} \times \tilde{\mathbb{P}})$ approximating $(X_t)_{t \in [0, T]}$ is given by⁴ \hat{X} . Moreover, this process is unique up to $(\mathbb{P} \times \tilde{\mathbb{P}})$ -null-sets.*

3 EXTENSION OF THE NEURAL JUMP ODE MODEL

After shortly revisiting the original Neural Jump ODE model and the definition of the signature transform of paths we introduce a signature based extension of NJ-ODE.

3.1 RECALL: NEURAL JUMP ODE

We define $\mathcal{X} \subset \mathbb{R}^{d_X}$ and $\mathcal{H} \subset \mathbb{R}^{d_H}$ to be the observation and latent spaces for $d_X, d_H \in \mathbb{N}$. Moreover, we define three feed-forward neural networks (with at least 1 hidden layer and e.g. sigmoid activation functions)

- $f_{\theta_1} : \mathbb{R}^{d_H} \times \mathbb{R}^{d_X} \times [0, T] \times [0, T] \rightarrow \mathbb{R}^{d_H}$ modelling the ODE dynamics,
- $\rho_{\theta_2} : \mathbb{R}^{d_X} \rightarrow \mathbb{R}^{d_H}$ modelling the jumps when new observations are made, and
- $g_{\theta_3} : \mathbb{R}^{d_H} \rightarrow \mathbb{R}^{d_Y}$ the readout map, mapping into the target space $\mathcal{Y} \subset \mathbb{R}^{d_Y}$ for $d_Y \in \mathbb{N}$,

where $\theta := (\theta_1, \theta_2, \theta_3) \in \Theta$ are the trainable weights. We define the pure jump stochastic process

$$u : \tilde{\Omega} \times [0, T] \rightarrow \mathbb{R}, (\tilde{\omega}, t) \mapsto u_t(\tilde{\omega}) := \sum_{i=1}^{n(\tilde{\omega})} \mathbf{1}_{[t_i(\tilde{\omega}), \infty)}(t). \quad (1)$$

Then the *Neural Jump ODE* (NJ-ODE) is defined by the latent process $H := (H_t)_{t \in [0, T]}$ and the output process $Y := (Y_t)_{t \in [0, T]}$ which are the solution of the SDE system

$$\begin{aligned} H_0 &= \rho_{\theta_2}(X_0), \\ dH_t &= f_{\theta_1}(H_{t-}, X_{\tau(t)}, \tau(t), t - \tau(t)) dt + (\rho_{\theta_2}(X_t) - H_{t-}) du_t, \\ Y_t &= g_{\theta_3}(H_t). \end{aligned} \quad (2)$$

The latent process H of the NJ-ODE before and after each observation can equivalently be written as

$$\begin{cases} h_{t_{i+1}-} & := \text{ODESolve}(f_{\theta_1}, (h_t, x_{t_i}, t_i, t - t_i), (t_i, t_{i+1})) \\ h_{t_{i+1}} & := \rho_{\theta_2}(x_{t_{i+1}}). \end{cases} \quad (3)$$

3.2 SIGNATURE TRANSFORM

The variation of a path is define as follows.

Definition 3.1. *Let J be a closed interval in \mathbb{R} and $d \geq 1$. Let $\mathbf{X} : J \rightarrow \mathbb{R}^d$ be a path on J . The variation of \mathbf{X} on the interval J is defined by*

$$\|\mathbf{X}\|_{var, J} = \sup_D \sum_{t_j \in D} |\mathbf{X}_{t_j} - \mathbf{X}_{t_{j-1}}|_1,$$

where the supremum is taken over all finite partitions D of J .

Remark 3.2. *We denote the set of \mathbb{R}^d -valued paths of bounded variation on J by $BV(J, \mathbb{R}^d)$. Endowed with the norm*

$$\|\mathbf{X}\|_{BV} := |\mathbf{X}_0|_1 + \|\mathbf{X}\|_{var, J}$$

$BV(J, \mathbb{R}^d)$ is a Banach space (Appell et al., 2013, Prop. 1.10).

For continuous paths of bounded variation we can define the signature transform.

⁴While we gave a pointwise definition, (Cohen & Elliott, 2015, Theorem 7.6.5) allows to define \hat{X} directly as the optional projection. By (Cohen & Elliott, 2015, Remark 7.2.2) this implies that the process \hat{X} is progressively measurable, in particular, jointly measurable in t and $\omega \times \tilde{\omega}$. However, as we have seen, even from the pointwise definition, it follows that \hat{X} is càdlàg, hence optional (Cohen & Elliott, 2015, Theorem 7.2.7).

Definition 3.3. Let J denote a closed interval in \mathbb{R} . Let $\mathbf{X} : J \rightarrow \mathbb{R}^d$ be a continuous path with finite variation. The signature of \mathbf{X} is defined as

$$S(\mathbf{X}) = (1, \mathbf{X}_J^1, \mathbf{X}_J^2, \dots),$$

where, for each $m \geq 1$,

$$\mathbf{X}_J^m = \int_{\substack{u_1 < \dots < u_m \\ u_1, \dots, u_m \in J}} d\mathbf{X}_{u_1} \otimes \dots \otimes d\mathbf{X}_{u_m} \in (\mathbb{R}^d)^{\otimes m}$$

is a collection of iterated integrals. The map from a path to its signature is called signature transform.

A good introduction to the signature transform with its properties and examples can be found in (Chevyrev & Kormilitzin, 2016; Kiraly & Oberhauser, 2019; Fermanian, 2020). In practice, we are not able to use the full (infinite) signature, but instead use a truncated version.

Definition 3.4. Let J denote a compact interval in \mathbb{R} . Let $\mathbf{X} : J \rightarrow \mathbb{R}^d$ be a continuous path with finite variation. The truncated signature of \mathbf{X} of order m is defined as follows

$$\pi_m(\mathbf{X}) = (1, \mathbf{X}_J^1, \mathbf{X}_J^2, \dots, \mathbf{X}_J^m),$$

i.e. the first $m + 1$ terms (levels) of the signature of \mathbf{X} .

Note that the size of the truncated signature depends on the dimension of \mathbf{X} , as well as the chosen level. Specifically, for a path of dimension d , the dimension of the truncated signature of order m is given by

$$\begin{cases} m + 1, & \text{if } d = 1, \\ \frac{d^{m+1} - 1}{d - 1}, & \text{if } d > 1. \end{cases} \quad (4)$$

When using the truncated signature as input to a model this results in a trade-off between accurately describing the path and model complexity.

For the following universality result of the signature we have to exclude tree like paths. Essentially, a path is tree-like, if it can be reduced to a constant path by successively removing pieces of the form $W * \overleftarrow{W}$, where \overleftarrow{W} is the time-reversal of W and $*$ the concatenation of paths.

Definition 3.5. A path $\mathbf{X} : [0, T] \rightarrow \mathbb{R}^d$ is tree-like if there exists a function $h : [0, T] \rightarrow [0, \infty)$ such that $h(0) = h(T) = 0$ and such that, for all $s, t \in [0, T]$ with $s \leq t$,

$$|\mathbf{X}_t - \mathbf{X}_s|_1 \leq h(s) + h(T) - 2 \inf_{u \in [s, t]} h(u).$$

Two paths are called tree-like equivalent if following forward the first one and concatenating with the backwards running second one leads to a tree-like path.

Remark 3.6. By adding time as one component to a given path, the set of tree-like equivalent paths reduces to a singleton.

For a Hilbert space \mathcal{H} we denote the set of continuous, \mathcal{H} -valued paths of bounded variation starting at the origin ($X_0 = 0$) on $[a, b]$ by $BV_0^c([a, b], \mathcal{H})$. The main reason why the signature transform is used, is its universal approximation property. It states that any continuous function invariant under tree-like equivalences of a path can be approximated arbitrarily well by a linear function of the truncated signature transform for some truncation level and is proven, e.g., in (Kiraly & Oberhauser, 2019, Theorem 1).

Theorem 3.7. Let \mathcal{P} be a compact subset of $BV_0^c([0, 1], \mathcal{H})$ of paths that are not tree-like equivalent. Let $f : \mathcal{P} \rightarrow \mathbb{R}$ be continuous in variation norm. Then, for any $\varepsilon > 0$, there exists $M > 0$ and a linear functional \mathbf{w} acting on the truncated signature of degree M such that

$$\sup_{\mathbf{x} \in \mathcal{P}} |f(\mathbf{x}) - \langle \mathbf{w}, \pi_M(\mathbf{x}) \rangle| < \varepsilon.$$

In the following proposition we show that the result of Theorem 3.7 can be extended to functions with additional inputs.

Proposition 3.8. *Let \mathcal{P} be a compact subset of $BV_0^c([0, 1], \mathcal{H})$ of paths that are not tree-like equivalent and let $C \subset \mathbb{R}^m$ for $m \in \mathbb{N}$ be compact. We consider the Cartesian product $BV_0^c([0, 1], \mathcal{H}) \times \mathbb{R}^m$ with the product norm given by the sum of the single norms (variation norm and 1-norm). Let $f : \mathcal{P} \times C \rightarrow \mathbb{R}$ be continuous. Then, for any $\varepsilon > 0$, there exists $M > 0$ and a continuous function \tilde{f} such that*

$$\sup_{(x,c) \in \mathcal{P} \times C} |f(x, c) - \tilde{f}(\pi_M(x), c)| < \varepsilon.$$

Remark 3.9. *We could with equal effort prove that there is a continuous selection of weights $c \mapsto \mathbf{w}(c)$ such that $\langle \mathbf{w}(c), \pi_M(\mathbf{x}) \rangle$ is close to $f(x, c)$ uniformly on compacts \mathcal{P} . For later purposes we shall need the proposition's assertion.*

Proof. Since f is a continuous function on a compact metric space, it is uniformly continuous by Heine-Cantor theorem. Hence, there exist $\delta > 0$ such that for all $c, \tilde{c} \in C$ with $|c - \tilde{c}| < \delta$ we have

$$|f(x, c) - f(x, \tilde{c})| < \varepsilon/2$$

for all $x \in \mathcal{P}$. Since C is compact, there exist finitely many open balls $(U_i)_{1 \leq i \leq N}$ with $U_i \subset \mathbb{R}^m$ of radius δ such that they cover C . Let the points $(c_i)_{1 \leq i \leq N} \in C^N$ be the centres of these balls. By the partition of unity, there exist continuous functions $(\rho_i)_{1 \leq i \leq N}$, with $\rho_i : C \rightarrow [0, 1]$ and $\text{supp}(\rho_i) \subset U_i$ such that $\sum_{i=1}^N \rho_i(c) = 1$ for all $c \in C$. For each c_i , Theorem 3.7 implies that there exist M_i and $\mathbf{w}_i \in \mathbb{R}^{M_i}$ such that the function $x \mapsto f(x, c_i)$ is approximated well by $\tilde{f}_i(\pi_{M_i}(x)) := \langle \mathbf{w}_i, \pi_{M_i}(x) \rangle$, i.e.

$$\sup_{x \in \mathcal{P}} |f(x, c_i) - \langle \mathbf{w}_i, \pi_{M_i}(x) \rangle| < \varepsilon/2.$$

W.l.o.g. we can assume that all $M_i = M$ are the same, by concatenating \mathbf{w}_i with 0s. Then the function $\tilde{f}(\pi_M(x), c) := \sum_{i=1}^N \rho_i(c) f_i(\pi_M(x))$ is continuous as sum of products of continuous functions and satisfies the claim. Indeed, for any $(x, c) \in \mathcal{P} \times C$ we have

$$\begin{aligned} |f(x, c) - \tilde{f}(\pi_M(x), c)| &= \left| \sum_{i=1}^N \rho_i(c) \left[f(x, c) - \tilde{f}_i(\pi_M(x)) \right] \right| \\ &\leq \sum_{i=1}^N \rho_i(c) |f(x, c) - \tilde{f}_i(\pi_M(x))| \\ &\leq \sum_{i=1}^N \rho_i(c) \left(|f(x, c) - f(x, c_i)| + |f(x, c_i) - \tilde{f}_i(\pi_M(x))| \right) \\ &\leq \sum_{i=1}^N \rho_i(c) (\varepsilon/2 + \varepsilon/2) \leq \varepsilon, \end{aligned}$$

where we used that $\rho_i(c) = 0$ if $c \notin U_i$ implying that $|c - c_i| < \delta$ if $\rho_i(c) > 0$ and therefore $|f(x, c) - f(x, c_i)| < \varepsilon/2$. \square

To apply this result, we need a tractable description of certain compact subsets of $BV_0^c([0, 1], \mathbb{R}^d)$ that include suitable paths for our considerations. Since $BV_0^c([0, 1], \mathbb{R}^d)$ is not finite dimensional, not every closed and bounded subset is compact. (Bugajewski & Gulowski, 2020, Theorem 2) characterizes relatively compact subsets of $BV_0^c([0, 1], \mathbb{R})$ (i.e. subsets such that their closure is compact). Moreover, they prove in (Bugajewski & Gulowski, 2020, Example 4), that the following set of functions is relatively compact.

Proposition 3.10. *For every $N \in \mathbb{N}$ the family $A_N \subset BV_0^c([0, 1], \mathbb{R})$ of all piecewise linear, bounded and continuous functions that can be written as*

$$f(t) = (a_1 t) \mathbf{1}_{[t_0, t_1]}(t) + \sum_{i=2}^N (a_i t + b_i) \mathbf{1}_{(t_{i-1}, t_i]}(t),$$

is relatively compact, where $a_i, b_i \in [-N, N]$, $b_1 = 0$, $a_i t_i = a_{i+1} t_i + b_{i+1}$, for all $1 \leq i \leq N$, and $0 = t_0 < t_1 < \dots < t_N = 1$.

The following remark shows that this result can be extended to \mathbb{R}^d -valued paths, which we will need for our considerations.

Remark 3.11. *Since the product of compact sets is compact and $BV_0^c([0, 1], \mathbb{R}^d)$ can be identified with $BV_0^c([0, 1], \mathbb{R})^d$, Proposition 3.10 can be extended to \mathbb{R}^d -valued paths. Moreover, the generalisation from $BV_0^c([0, 1], \mathbb{R}^d)$ to $BV_0^c([0, T], \mathbb{R}^d)$ is immediate. These are the compact subsets A_N of $BV_0^c([0, T], \mathbb{R}^d)$ that we will use.*

3.3 PATH-DEPENDENT NEURAL JUMP ODE

We adapt (2) by using the signature as additional input in the neural ODE f_{θ_1} as well as the jump network ρ_{θ_2} . Moreover, since the process X is not necessarily Markovian any more, we go back to a recurrent structure for the jump network ρ_{θ_2} , as in (Brouwer et al., 2019; Rubanova et al., 2019). Note that we cannot use the signature of the true path $(X_s)_{0 \leq s \leq t}$ of the data up to time t as input, since we only have discrete observations of X at the observation times t_i (which is not sufficient to calculate the signature of X). Instead, we use the shifted interpolation $\tilde{X}^{\leq t} - X_0 \in BV_0^c([0, T])$ up to time t and compute the truncated signature $\pi_n(\tilde{X}^{\leq t} - X_0)$. This signature together with the starting point X_0 include all available information (while the signature of $(X_s)_{0 \leq s \leq t}$ would include much more than the available information, i.e., it is not \mathcal{A}_t -measurable). Moreover, the interpolation $\tilde{X}^{\leq t}$ has bounded variation, no matter whether this is true for the original path X or not. Hence, Theorem 3.7 applies if $\tilde{X}^{\leq t}$ lies in some compact subset. The advantage (besides Theorem 3.7) of using the truncated signature over using the discrete observations directly is, that the truncated signature cumulates information of an arbitrary number of observations in a vector of fixed size.

Definition 3.12. *The path-dependent neural jump ODE (PD-NJ-ODE) model (of order $n \in \mathbb{N}$) is given by*

$$\begin{aligned} H_0 &= \rho_{\theta_2}(0, 0, \pi_n(0), X_0), \\ dH_t &= f_{\theta_1}\left(H_{t-}, t, \tau(t), \pi_n(\tilde{X}^{\leq \tau(t)} - X_0), X_0\right) dt \\ &\quad + \left(\rho_{\theta_2}\left(H_{t-}, t, \pi_n(\tilde{X}^{\leq \tau(t)} - X_0), X_0\right) - H_{t-}\right) du_t, \\ Y_t &= g_{\theta_3}(H_t). \end{aligned} \tag{5}$$

The functions f_{θ_1} , ρ_{θ_2} and g_{θ_3} are feedforward neural networks with parameters $\theta = (\theta_1, \theta_2, \theta_3) \in \Theta$ and u is the jump process counting the observations defined in (1).

(Protter, 2005, Thm. 7, Chap. V) implies that a unique solution of (5) exists. We write $Y^\theta(X)$ to emphasize the dependence of Y on θ and X .

3.3.1 OBJECTIVE FUNCTION

Let \mathbb{D} to be the set of all $\mathbb{R}^{d \times d}$ -valued \mathbb{A} -adapted processes on the probability space $(\Omega \times \tilde{\Omega}, \mathcal{F} \otimes \tilde{\mathcal{F}}, \mathbb{P} \otimes \tilde{\mathbb{P}})$. Then we define our objective functions

$$\begin{aligned} \Psi : \mathbb{D} &\rightarrow \mathbb{R}, \\ Z &\mapsto \Psi(Z) := \mathbb{E}_{\mathbb{P} \times \tilde{\mathbb{P}}} \left[\frac{1}{n} \sum_{i=1}^n (|M_i \odot (X_{t_i} - Z_{t_i})|_2 + |M_i \odot (Z_{t_i} - Z_{t_i-})|_2)^2 \right], \end{aligned} \tag{6}$$

$$\Phi : \Theta \rightarrow \mathbb{R}, \theta \mapsto \Phi(\theta) := \Psi(Y^\theta(X)), \tag{7}$$

where \odot is the element-wise multiplication (Hadamard product) and Φ will be our (theoretical) loss function. Remark that from the definition of Y^θ it directly follows that it is an element of \mathbb{D} , hence Φ is well-defined.

Let us assume, that we observe $N \in \mathbb{N}$ independent realisations of the path X together with independent realizations of the observation mask M at times $(t_1^{(j)}, \dots, t_{n_j}^{(j)})$, $1 \leq j \leq N$, which are themselves independent realisations of the random vector (n, t_1, \dots, t_n) . In particular, let us assume that $X^{(j)} \sim X$, $M^{(j)} \sim M$ and $(n^j, t_1^{(j)}, \dots, t_{n_j}^{(j)}) \sim (n, t_1, \dots, t_{n_j})$ are i.i.d. random processes

(respectively variables) for $1 \leq j \leq N$ and that our training data is one realisation of them. We write $Y^{\theta,j} := Y^{\theta}(X^{(j)})$. Then the Monte Carlo approximation of our loss function

$$\hat{\Phi}_N(\theta) := \frac{1}{N} \sum_{j=1}^N \frac{1}{n^j} \sum_{i=1}^{n^j} \left(\left| M_i^{(j)} \odot \left(X_{t_i^{(j)}}^{(j)} - Y_{t_i^{(j)}}^{\theta,j} \right) \right|_2 + \left| M_i^{(j)} \odot \left(Y_{t_i^{(j)}}^{\theta,j} - Y_{t_i^{(j)-}}^{\theta,j} \right) \right|_2 \right)^2, \quad (8)$$

converges $(\mathbb{P} \times \tilde{\mathbb{P}})$ -a.s. to $\Phi(\theta)$ as $N \rightarrow \infty$, by the law of large numbers (cf. Theorem 4.3).

4 CONVERGENCE GUARANTEES

As in (Herrera et al., 2021), we first give the convergence result for the objective function Φ and then show that its Monte Carlo approximation $\hat{\Phi}$ converges to it. The proofs mainly follow the proofs therein, with extensions for the more general setting. Let Θ_m be the set of possible weights for the 3 neural networks, such that their widths are at most m and such that the truncated signature of level m or smaller is used.

4.1 CONVERGENCE OF THEORETICAL LOSS FUNCTION

Theorem 4.1. *Let $\theta_m^{\min} \in \Theta_m^{\min} := \operatorname{argmin}_{\theta \in \Theta_m} \{\Phi(\theta)\}$ for every $m \in \mathbb{N}$. If Assumption 2.1 is satisfied, then, for $m \rightarrow \infty$, the value of the loss function Φ (7) converges to the minimal value of Ψ (6) which is uniquely achieved by \hat{X} , i.e.*

$$\Phi(\theta_m^{\min}) \xrightarrow{m \rightarrow \infty} \min_{Z \in \mathbb{D}} \Psi(Z) = \Psi(\hat{X}).$$

Furthermore, for every $1 \leq k \leq K$ we have that $Y^{\theta_m^{\min}}$ converges to \hat{X} as a random variable in $L^1(\Omega \times [0, T], \mathbb{P} \times \lambda_k)$. In particular, the limit process $Y := \lim_{m \rightarrow \infty} Y^{\theta_m^{\min}}$ equals \hat{X} $(\mathbb{P} \times \lambda_k)$ -almost surely as a random variable on $\Omega \times [0, T]$.

Before proving the theorem, we derive the following useful result, which is an extension of a result in (Herrera et al., 2021).

Lemma 4.2. *For any \mathbb{A} -adapted process Z it holds that*

$$\begin{aligned} \mathbb{E}_{\mathbb{P} \times \tilde{\mathbb{P}}} \left[\frac{1}{n} \sum_{i=1}^n \left| M_{t_i} \odot (X_{t_i} - Z_{t_i-}) \right|_2^2 \right] \\ = \mathbb{E}_{\mathbb{P} \times \tilde{\mathbb{P}}} \left[\frac{1}{n} \sum_{i=1}^n \left| M_{t_i} \odot (X_{t_i} - \hat{X}_{t_i-}) \right|_2^2 \right] + \mathbb{E}_{\mathbb{P} \times \tilde{\mathbb{P}}} \left[\frac{1}{n} \sum_{i=1}^n \left| M_{t_i} \odot (\hat{X}_{t_i-} - Z_{t_i-}) \right|_2^2 \right]. \end{aligned}$$

Proof. First note that by Assumption 2.1 3. we have that $X_{t_i} = X_{t_i-}$ almost surely. Then

$$\begin{aligned} \mathbb{E}_{\mathbb{P} \times \tilde{\mathbb{P}}} \left[\frac{1}{n} \sum_{i=1}^n \left| M_{t_i} \odot (X_{t_i-} - Z_{t_i-}) \right|_2^2 \right] &= \mathbb{E}_{\tilde{\mathbb{P}}} \left[\frac{1}{n} \sum_{i=1}^n \sum_{j=1}^{d_X} M_{t_i,j} \mathbb{E}_{\mathbb{P}} \left[|X_{t_i-,j} - Z_{t_i-,j}|^2 \right] \right] \\ &= \mathbb{E}_{\tilde{\mathbb{P}}} \left[\frac{1}{n} \sum_{i=1}^n \sum_{j=1}^{d_X} M_{t_i,j} \left(\mathbb{E}_{\mathbb{P}} \left[|X_{t_i-,j} - \hat{X}_{t_i-,j}|^2 \right] + \mathbb{E}_{\mathbb{P}} \left[|(\hat{X}_{t_i-,j} - Z_{t_i-,j})|^2 \right] \right) \right] \\ &= \mathbb{E}_{\mathbb{P} \times \tilde{\mathbb{P}}} \left[\frac{1}{n} \sum_{i=1}^n \left| M_{t_i} \odot (X_{t_i-} - \hat{X}_{t_i-}) \right|_2^2 \right] + \mathbb{E}_{\mathbb{P} \times \tilde{\mathbb{P}}} \left[\frac{1}{n} \sum_{i=1}^n \left| M_{t_i} \odot (\hat{X}_{t_i-} - Z_{t_i-}) \right|_2^2 \right], \end{aligned}$$

where we used (Herrera et al., 2021, Proposition B.2, Lemma B.3) and Fubini's theorem. \square

Proof of Theorem 4.1. We start by showing that $\hat{X} \in \mathbb{D}$ is the unique minimizer of Ψ up to $(\mathbb{P} \times \lambda_k)$ -null-sets for any $k \leq K$. First, note that for every t_i we have $M_{t_i} \odot \hat{X}_{t_i} = M_{t_i} \odot X_{t_i}$ and that

$X_{t_i} = X_{t_{i-}}$ if $t_i \notin \mathcal{J}$, hence with probability 1. Therefore,

$$\begin{aligned} \Psi(\hat{X}) &= \mathbb{E}_{\mathbb{P} \times \tilde{\mathbb{P}}} \left[\frac{1}{n} \sum_{i=1}^n |M_{t_i} \odot (X_{t_i} - \hat{X}_{t_{i-}})|_2^2 \right] \\ &= \min_{Z \in \mathbb{D}} \mathbb{E}_{\mathbb{P} \times \tilde{\mathbb{P}}} \left[\frac{1}{n} \sum_{i=1}^n |M_{t_i} \odot (X_{t_i} - Z_{t_{i-}})|_2^2 \right] \\ &\leq \min_{Z \in \mathbb{D}} \mathbb{E}_{\mathbb{P} \times \tilde{\mathbb{P}}} \left[\frac{1}{n} \sum_{i=1}^n (|M_{t_i} \odot (X_{t_i} - Z_{t_i})|_2 + |M_{t_i} \odot (Z_{t_i} - Z_{t_{i-}})|_2)^2 \right] \\ &= \min_{Z \in \mathbb{D}} \Psi(Z), \end{aligned}$$

where we use Lemma 4.2 for the second line and the triangle inequality for the third line. Hence, \hat{X} is a minimizer of Ψ .

To see that it is unique ($\mathbb{P} \times \lambda_k$)-a.s., let $Z \in \mathbb{D}$ be a process such that $(\mathbb{P} \times \lambda_k)[\hat{X} \neq Z] > 0$. By (Herrera et al., 2021, Lemma E.4), this implies that there exists an $\varepsilon > 0$ such that $B := \{t \in [0, T] \mid \mathbb{E}_{\mathbb{P}}[|X_{t-} - Z_{t-}|_2^2] \geq \varepsilon + \mathbb{E}_{\mathbb{P}}[|X_{t-} - \hat{X}_{t-}|_2^2]\}$ satisfies $\lambda_k(B) > 0$. For $1 \leq \ell \leq d_X$, let $B_\ell := \{t- \in B \mid \mathbb{E}_{\mathbb{P}}[|X_{t-, \ell} - Z_{t-, \ell}|^2] \geq \varepsilon/d_X + \mathbb{E}_{\mathbb{P}}[|X_{t-, \ell} - \hat{X}_{t-, \ell}|^2]\}$, then an easy argument by contradiction shows that $B = \cup_{1 \leq \ell \leq d_X} B_\ell$. Since $0 < \lambda_k(B) \leq \sum_{\ell} \lambda_k(B_\ell)$, there exists some $1 \leq \ell \leq d_X$ such that $\lambda_k(B_\ell) > 0$. Now recall that by definition of λ_k we have $\lambda_k(B_\ell) = \tilde{\mathbb{P}}(\dot{\cup}_{j \geq k} \{n = j, t_k- \in B_\ell\}) / \tilde{\mathbb{P}}(n \geq k) > 0$. This implies that there exists $j \in \mathbb{N}_{\geq k}$ such that $\tilde{\mathbb{P}}(n = j, t_k- \in B_\ell) > 0$. Therefore,

$$\begin{aligned} \mathbb{E}_{\tilde{\mathbb{P}}} \left[\frac{1}{n} \sum_{i=1}^n M_{t_i, \ell} \mathbf{1}_{\{t_i- \in B_\ell\}} \right] &\geq \mathbb{E}_{\tilde{\mathbb{P}}} \left[\mathbf{1}_{\{n=j\}} \frac{1}{n} \sum_{i=1}^n M_{t_i, \ell} \mathbf{1}_{\{t_i- \in B_\ell\}} \right] \\ &\geq \mathbb{E}_{\tilde{\mathbb{P}}} \left[\mathbf{1}_{\{n=j\}} \frac{1}{j} M_{t_k, \ell} \mathbf{1}_{\{t_k- \in B_\ell\}} \right] \\ &= \mathbb{E}_{\tilde{\mathbb{P}}} \left[\mathbf{1}_{\{n=j\}} \frac{1}{j} \mathbf{1}_{\{t_k- \in B_\ell\}} \right] \mathbb{E}_{\tilde{\mathbb{P}}} \left[\mathbf{1}_{\{M_{t_k, \ell} = 1\}} \right] \\ &= \frac{1}{j} \tilde{\mathbb{P}}(n = j, t_k- \in B_\ell) \tilde{\mathbb{P}}(M_{t_k, \ell} = 1) > 0, \end{aligned}$$

where we used (Assumption 2.1 1.) in the third and the last line. This inequality implies now that Z is not a minimizer of Ψ , because

$$\begin{aligned} \Psi(Z) &= \mathbb{E}_{\mathbb{P} \times \tilde{\mathbb{P}}} \left[\frac{1}{n} \sum_{i=1}^n (|M_{t_i} \odot (X_{t_i} - Z_{t_i})|_2 + |M_{t_i} \odot (Z_{t_i} - Z_{t_{i-}})|_2)^2 \right] \\ &\geq \mathbb{E}_{\tilde{\mathbb{P}}} \left[\frac{1}{n} \sum_{i=1}^n \mathbb{E}_{\mathbb{P}} \left[|M_{t_i} \odot (X_{t_i} - Z_{t_{i-}})|_2^2 \right] \right] \\ &= \mathbb{E}_{\tilde{\mathbb{P}}} \left[\frac{1}{n} \sum_{i=1}^n \left(\mathbf{1}_{\{t_i- \in B_\ell\}} + \mathbf{1}_{\{t_i- \in B_\ell^c\}} \right) \mathbb{E}_{\mathbb{P}} \left[|M_{t_i} \odot (X_{t_i} - Z_{t_{i-}})|_2^2 \right] \right] \\ &\geq \mathbb{E}_{\tilde{\mathbb{P}}} \left[\frac{1}{n} \sum_{i=1}^n \left(M_{t_i, \ell} \frac{\varepsilon}{d_X} \mathbf{1}_{\{t_i- \in B_\ell\}} + \mathbb{E}_{\mathbb{P}} \left[|M_{t_i} \odot (X_{t_i} - \hat{X}_{t_{i-}})|_2^2 \right] \right) \right] \\ &= \varepsilon \mathbb{E}_{\tilde{\mathbb{P}}} \left[\frac{1}{n} \sum_{i=1}^n M_{t_i, \ell} \mathbf{1}_{\{t_i- \in B_\ell\}} \right] + \min_{Z \in \mathbb{D}} \Psi(Z) \\ &> \min_{Z \in \mathbb{D}} \Psi(Z). \end{aligned}$$

Next we show that (5) can approximate \hat{X} arbitrarily well. Since the dimension d_H can be chosen freely, let us fix it to $d_H := d_X$. Furthermore, let us fix $\theta_3^{*,m}$ such that $g_{\theta_3^{*,m}} = \text{id}$. Let $\varepsilon > 0$, $(N_\varepsilon)_{\varepsilon > 0}$ a monotone sequence (defined below) in \mathbb{N} with $\lim_{\varepsilon \rightarrow 0} N_\varepsilon = \infty$ and \mathcal{P}_ε be the closure of the set A_{N_ε} of Remark 3.11, which is compact. For any $1 \leq j \leq d_X$, the function f_j is continuous by

Assumption 2.1 and can equivalently be written as (continuous) function $\hat{f}_j(t, \tau(t), \tilde{X}^{\leq \tau(t)} - X_0, X_0)$. Therefore, Proposition 3.8 implies that there exists an $m_\varepsilon \in \mathbb{N}$ and a continuous function \tilde{f}_j such that

$$\sup_{(t, \tau, X) \in [0, T]^2 \times \mathcal{P}_\varepsilon} \left| f_j(t, \tau, X) - \tilde{f}_j(t, \tau, \pi_{m_\varepsilon}(X - X_0), X_0) \right| \leq \varepsilon/2.$$

Since the variation of functions in \mathcal{P}_ε is uniformly bounded by a finite constant, the set of their truncated signatures $\pi_{m_\varepsilon}(\mathcal{P}_\varepsilon)$ is a bounded subset in \mathbb{R}^d for some $d \in \mathbb{N}$ (depending on d_X and m_ε), hence its closure, denoted by Π_ε , is compact. Therefore, the universal approximation theorem for neural networks (Hornik et al., 1989, Theorem 2.4) implies that there exists an $m \in \mathbb{N}$ and neural network weights $\theta_1^{*,m} \in \Theta_m^1$ such that for every $1 \leq j \leq d_X$ the function \tilde{f}_j is approximated up to $\varepsilon/2$ by the j -th coordinate of the neural network $f_{\theta_1^{*,m}}$ (denoted by $f_{\theta_1^{*,m},j}$) on the compact set $[0, T]^2 \times \Pi_\varepsilon$. Hence, combining the two approximations we get (by triangle inequality)

$$\sup_{(t, \tau, X) \in [0, T]^2 \times \mathcal{P}_\varepsilon} \left| f_j(t, \tau, X) - f_{\theta_1^{*,m},j}(t, \tau, \pi_{m_\varepsilon}(X - X_0), X_0) \right| \leq \varepsilon.$$

Obviously, extending the input of the neural network does not make the approximation worse, by simply setting the corresponding weights to 0, hence, also H_{t-} can be used as additional input. Moreover, it is easy to see that without loss of generality $m = m_\varepsilon$ can be assumed (by increasing the smaller of the two). Similarly we get that there exists an $m \in \mathbb{N}$ and neural network weights $\theta_2^{*,m} \in \Theta_m^2$ such that for every $1 \leq j \leq d_X$

$$\sup_{(t, X) \in [0, T] \times \mathcal{P}_\varepsilon} \left| F_j(t, t, X) - \rho_{\theta_2^{*,m},j}(t, \pi_m(X - X_0), X_0) \right| \leq \varepsilon.$$

As for f , H_{t-} can be used as additional input without worsening the approximation. Since F_j, f_j are bounded by $B(X_T^* + 1)^p$ (Assumption 2.1 4.), we can bound the neural networks $f_{\theta_1^{*,m}}, \rho_{\theta_2^{*,m}}$ by $B(X_T^* + 1)^p + \varepsilon$ in a way, such that the resulting function is still continuous. Indeed, we can use the minimum of the neural network output and the maximum norm of the neural network output on the compact set $[0, T]^2 \times \Pi_\varepsilon$, which is naturally bounded by $B(X_T^* + 1)^p + \varepsilon$. Note that the resulting functions still satisfy the same approximation bounds. By abuse of notation we call these functions again $f_{\theta_1^{*,m}}, \rho_{\theta_2^{*,m}}$ and use them whenever we speak of neural networks. In particular, we have the global bounds $\|f_j - f_{\theta_1^{*,m},j}\|_\infty \leq 2B(X_T^* + 1)^p$ and $|F_j - \rho_{\theta_2^{*,m},j}|_\infty \leq 2B(X_T^* + 1)^p$.

Now we can bound the distance between $Y_t^{\theta_m^*}$ and \hat{X} , where $\theta_m^* := (\theta_1^{*,m}, \theta_2^{*,m}, \theta_3^{*,m})$. Whenever $X_T^* < 1/\varepsilon$, the number of observations satisfies $n < 1/\varepsilon$ and the minimal difference between any two consecutive observation times $\delta > \varepsilon$, we know that the corresponding path $\tilde{X}^{\leq \tau(t)} - X_0$ is an element of A_{N_ε} for $N_\varepsilon := \lceil 2(T+1)\varepsilon^{-2} \rceil$ and therefore, the neural network approximations up to ε hold. Otherwise, one of those conditions is not satisfied and the global upper bound can be used. Hence, if $t \in \{t_1, \dots, t_n\}$, we have for $F = (F_j)_{1 \leq j \leq d_X}$ and $f = (f_j)_{1 \leq j \leq d_X}$

$$\begin{aligned} \left| Y_t^{\theta_m^*} - \hat{X}_t \right|_1 &= \left| \rho_{\theta_2^{*,m}}(H_{t-}, t, \pi_m(\tilde{X}^{\leq t} - X_0), X_0) - F(t, t, \tilde{X}^{\leq t}) \right|_1 \\ &\leq \varepsilon d_X \mathbf{1}_{\{X_T^* < 1/\varepsilon\}} \mathbf{1}_{\{n < 1/\varepsilon\}} \mathbf{1}_{\{\delta > \varepsilon\}} \\ &\quad + 2d_X B(X_T^* + 1)^p \left(\mathbf{1}_{\{X_T^* \geq 1/\varepsilon\}} + \mathbf{1}_{\{n \geq 1/\varepsilon\}} + \mathbf{1}_{\{\delta \leq \varepsilon\}} \right), \end{aligned}$$

and if $t \notin \{t_1, \dots, t_n\}$,

$$\begin{aligned} \left| Y_t^{\theta_m^*} - \hat{X}_t \right|_1 &\leq \left| Y_{\tau(t)}^{\theta_m^*} - \hat{X}_{\tau(t)} \right|_1 \\ &\quad + \int_{\tau(t)}^t \left| f_{\theta_1} \left(H_{s-}, s, \tau(t), \pi_m(\tilde{X}^{\leq \tau(t)} - X_0), X_0 \right) - f(s, \tau(t), \tilde{X}^{\leq \tau(t)}) \right|_1 ds \\ &\leq \varepsilon(T+1)d_X \mathbf{1}_{\{X_T^* < 1/\varepsilon\}} \mathbf{1}_{\{n < 1/\varepsilon\}} \mathbf{1}_{\{\delta > \varepsilon\}} \\ &\quad + 2(T+1)d_X B(X_T^* + 1)^p \left(\mathbf{1}_{\{X_T^* \geq 1/\varepsilon\}} + \mathbf{1}_{\{n \geq 1/\varepsilon\}} + \mathbf{1}_{\{\delta \leq \varepsilon\}} \right). \end{aligned}$$

Moreover, by equivalence of the 1- and 2-norm, there exists a constant $c > 0$ such that for all $t \in [0, T]$

$$\begin{aligned} \left| Y_t^{\theta_m^*} - \hat{X}_t \right|_2 &\leq c\varepsilon(T+1)d_X + 2c(T+1)d_X B(X_T^* + 1)^p \left(\mathbf{1}_{\{X_T^* \geq 1/\varepsilon\}} + \mathbf{1}_{\{n \geq 1/\varepsilon\}} + \mathbf{1}_{\{\delta \leq \varepsilon\}} \right) \\ &=: c_m. \end{aligned}$$

So far, we have fixed an $\varepsilon > 0$ and argued that there exist $m \in \mathbb{N}$ such that the neural network approximation bounds hold. On the other hand it is clear, that increasing m only makes the approximations better, hence, there exists a decreasing sequence $(\varepsilon_m)_{m \geq 0}$, with $\lim_{m \rightarrow \infty} \varepsilon_m = 0$, such that the above approximations hold with error ε_m for any given truncation level and network size $m \in \mathbb{N}$, where θ_m^* is always chosen to approximate the functions as good as possible. Note that Assumption 2.1 implies that there exists $C > 0$ such that $\mathbb{E}_{\mathbb{P}}[|X_{t_i} - \hat{X}_{t_i-}|_2^2] < C$ and that $M_{t_i} \odot \hat{X}_{t_i} = M_{t_i} \odot X_{t_i}$. Since θ_m^{\min} is chosen to minimize the loss function for the given truncation level and network size $m \in \mathbb{N}$, we get

$$\begin{aligned}
\min_{Z \in \mathbb{D}} \Psi(Z) &\leq \Phi(\theta_m^{\min}) \leq \Phi(\theta_m^*) \\
&= \mathbb{E}_{\mathbb{P} \times \tilde{\mathbb{P}}} \left[\frac{1}{n} \sum_{i=1}^n \left(\left| M_{t_i} \odot (X_{t_i} - Y_{t_i}^{\theta_m^*}) \right|_2 + \left| M_{t_i} \odot (Y_{t_i}^{\theta_m^*} - Y_{t_i-}^{\theta_m^*}) \right|_2 \right)^2 \right] \\
&\leq \mathbb{E}_{\mathbb{P} \times \tilde{\mathbb{P}}} \left[\frac{1}{n} \sum_{i=1}^n \left(\left| M_{t_i} \odot (\hat{X}_{t_i} - Y_{t_i}^{\theta_m^*}) \right|_2 + \left| M_{t_i} \odot (Y_{t_i}^{\theta_m^*} - \hat{X}_{t_i}) \right|_2 \right. \right. \\
&\quad \left. \left. + \left| M_{t_i} \odot (\hat{X}_{t_i} - \hat{X}_{t_i-}) \right|_2 + \left| M_{t_i} \odot (\hat{X}_{t_i-} - Y_{t_i-}^{\theta_m^*}) \right|_2 \right)^2 \right] \\
&\leq \mathbb{E}_{\mathbb{P} \times \tilde{\mathbb{P}}} \left[\frac{1}{n} \sum_{i=1}^n \left(\left| M_{t_i} \odot (X_{t_i} - \hat{X}_{t_i-}) \right|_2 + 3c_m \right)^2 \right] \tag{9} \\
&\leq \mathbb{E}_{\tilde{\mathbb{P}}} \left[\frac{1}{n} \sum_{i=1}^n \mathbb{E}_{\mathbb{P}} \left[\left(\left| M_{t_i} \odot (X_{t_i} - \hat{X}_{t_i-}) \right|_2 + 3c_m \right)^2 \right] \right] \\
&\leq \mathbb{E}_{\tilde{\mathbb{P}}} \left[\frac{1}{n} \sum_{i=1}^n \left(\mathbb{E}_{\mathbb{P}} \left[\left| M_{t_i} \odot (X_{t_i} - \hat{X}_{t_i-}) \right|_2^2 \right]^{1/2} + \mathbb{E}_{\mathbb{P}} [9c_m^2]^{1/2} \right)^2 \right] \\
&\leq \mathbb{E}_{\tilde{\mathbb{P}}} \left[\frac{1}{n} \sum_{i=1}^n \left(\mathbb{E}_{\mathbb{P}} \left[\left| M_{t_i} \odot (X_{t_i} - \hat{X}_{t_i-}) \right|_2^2 \right] + \mathbb{E}_{\mathbb{P}} [9c_m^2] + 6\mathbb{E}_{\mathbb{P}} [c_m^2]^{1/2} C^{1/2} \right) \right] \\
&\leq \Psi(\hat{X}) + c \left(\mathbb{E}_{\mathbb{P} \times \tilde{\mathbb{P}}} [c_m^2] + \mathbb{E}_{\mathbb{P} \times \tilde{\mathbb{P}}} [c_m^2]^{1/2} \right)
\end{aligned}$$

where we used the triangle inequality for the L^2 -norm in the 5th line and $c > 0$ is a suitable constant. Integrability of $|X_T^*|_2$ and $|n|$ together with the assumption on δ imply that

$$\mathbf{1}_{\{X_T^* \geq 1/\varepsilon_m\}} + \mathbf{1}_{\{n \geq 1/\varepsilon_m\}} + \mathbf{1}_{\{\delta \leq \varepsilon_m\}} \xrightarrow[m \rightarrow \infty]{\mathbb{P} \times \tilde{\mathbb{P}}\text{-a.s.}} 0.$$

Therefore, we have for a suitable constant $c > 0$ (not depending on ε_m and m),

$$\mathbb{E}_{\mathbb{P} \times \tilde{\mathbb{P}}} [c_m^2] \leq c\varepsilon_m^2 + c\mathbb{E}_{\mathbb{P} \times \tilde{\mathbb{P}}} \left[(X_T^* + 1)^{2p} \left(\mathbf{1}_{\{X_T^* \geq 1/\varepsilon_m\}} + \mathbf{1}_{\{n \geq 1/\varepsilon_m\}} + \mathbf{1}_{\{\delta \leq \varepsilon_m\}} \right) \right] \xrightarrow{m \rightarrow \infty} 0,$$

by dominated convergence, since X_T^* is L^{2p} -integrable by Assumption 2.1. Using this and $\Psi(\hat{X}) = \min_{Z \in \mathbb{D}} \Psi(Z)$, we get from (9)

$$\min_{Z \in \mathbb{D}} \Psi(Z) \leq \Phi(\theta_m^{\min}) \leq \Phi(\theta_m^*) \xrightarrow{m \rightarrow \infty} \min_{Z \in \mathbb{D}} \Psi(Z).$$

Finally, we show that the limits $\lim_{m \rightarrow \infty} Y^{\theta_m^{\min}}$ and $\lim_{m \rightarrow \infty} Y^{\theta_m^*}$ exist as limits in the Banach space $\mathbb{L} := L^1(\Omega \times [0, T], \mathbb{F} \otimes \mathcal{B}([0, T]), \mathbb{P} \times \lambda_k)$, for every $k \leq K$, and that they are both equal to \hat{X} . Let us fix $k \leq K$. As was shown in (Herrera et al., 2021), we have for $c := (\mathbb{P}(n \geq k))^{-1}$ and a $\mathcal{B}([0, T])$ -measurable function $Z : [0, T] \rightarrow \mathbb{R}$, $t \mapsto Z_t := Z(t)$ that

$$\mathbb{E}_{\lambda_k} [Z] = c\mathbb{E}_{\tilde{\mathbb{P}}} [\mathbf{1}_{\{n \geq k\}} Z_{t_k-}]. \tag{10}$$

Moreover, the triangle inequality and Lemma 4.2 yield

$$\begin{aligned}
\Phi(\theta_m^*) - \Psi(\hat{X}) &\geq \mathbb{E}_{\mathbb{P} \times \tilde{\mathbb{P}}} \left[\frac{1}{n} \sum_{i=1}^n \left| M_{t_i} \odot (X_{t_i} - Y_{t_i-}^{\theta_m^*}) \right|_2^2 \right] - \Psi(\hat{X}) \\
&= \mathbb{E}_{\mathbb{P} \times \tilde{\mathbb{P}}} \left[\frac{1}{n} \sum_{i=1}^n \left| M_{t_i} \odot (\hat{X}_{t_i-} - Y_{t_i-}^{\theta_m^*}) \right|_2^2 \right]. \tag{11}
\end{aligned}$$

For any \mathbb{R}^{d_X} -valued $Z \in \mathbb{L}$ the Hölder inequality, together with the fact that $n \geq 1$, yields

$$\mathbb{E}_{\mathbb{P} \times \tilde{\mathbb{P}}} [|Z|_2] = \mathbb{E}_{\mathbb{P} \times \tilde{\mathbb{P}}} \left[\frac{\sqrt{n}}{\sqrt{n}} |Z|_2 \right] \leq \mathbb{E}_{\mathbb{P} \times \tilde{\mathbb{P}}} [n]^{1/2} \mathbb{E}_{\mathbb{P} \times \tilde{\mathbb{P}}} \left[\frac{1}{n} |Z|_2^2 \right]^{1/2}. \quad (12)$$

By Assumption 2.1 1., we know that $\mu := \min_{1 \leq j \leq d_X} \tilde{\mathbb{P}}(M_{k,j} = 1) > 0$. Hence, we have by the independence of $M_{k,j}$ from t_k and n that

$$\begin{aligned} \mathbb{E}_{\mathbb{P} \times \tilde{\mathbb{P}}} \left[\mathbf{1}_{\{n \geq k\}} \left| M_{t_k} \odot (\hat{X}_{t_k-} - Y_{t_k-}^{\theta_m^*}) \right|_1 \right] &= \mathbb{E}_{\mathbb{P} \times \tilde{\mathbb{P}}} \left[\mathbf{1}_{\{n \geq k\}} \sum_{j=1}^{d_X} M_{k,j} \left| \hat{X}_{t_k-,j} - Y_{t_k-,j}^{\theta_m^*} \right| \right] \\ &= \sum_{j=1}^{d_X} \mathbb{E}_{\mathbb{P} \times \tilde{\mathbb{P}}} [M_{k,j}] \mathbb{E}_{\mathbb{P} \times \tilde{\mathbb{P}}} \left[\mathbf{1}_{\{n \geq k\}} \left| \hat{X}_{t_k-,j} - Y_{t_k-,j}^{\theta_m^*} \right| \right] \geq \mu \mathbb{E}_{\mathbb{P} \times \tilde{\mathbb{P}}} \left[\mathbf{1}_{\{n \geq k\}} \left| \hat{X}_{t_k-} - Y_{t_k-}^{\theta_m^*} \right|_1 \right] \end{aligned}$$

and by the the equivalence of 1- and 2-norm, we therefore have for some constant $\hat{c} > 0$

$$\mathbb{E}_{\mathbb{P} \times \tilde{\mathbb{P}}} \left[\mathbf{1}_{\{n \geq k\}} \left| \hat{X}_{t_k-} - Y_{t_k-}^{\theta_m^*} \right|_2 \right] \leq \frac{\hat{c}}{\mu} \mathbb{E}_{\mathbb{P} \times \tilde{\mathbb{P}}} \left[\mathbf{1}_{\{n \geq k\}} \left| M_{t_k} \odot (\hat{X}_{t_k-} - Y_{t_k-}^{\theta_m^*}) \right|_2 \right]. \quad (13)$$

Together, this implies that $\lim_{m \rightarrow \infty} Y^{\theta_m^*} = \hat{X}$ as a \mathbb{L} -limit. Indeed, with $\tilde{c} := \mathbb{E}_{\mathbb{P} \times \tilde{\mathbb{P}}} [n]^{1/2} < \infty$ we have

$$\begin{aligned} \mathbb{E}_{\mathbb{P} \times \lambda_k} \left[\left| \hat{X} - Y^{\theta_m^*} \right|_2 \right] &= c \mathbb{E}_{\mathbb{P} \times \tilde{\mathbb{P}}} \left[\mathbf{1}_{\{n \geq k\}} \left| \hat{X}_{t_k-} - Y_{t_k-}^{\theta_m^*} \right|_2 \right] \\ &= \frac{c \hat{c}}{\mu} \mathbb{E}_{\mathbb{P} \times \tilde{\mathbb{P}}} \left[\mathbf{1}_{\{n \geq k\}} \left| M_{t_k} \odot (\hat{X}_{t_k-} - Y_{t_k-}^{\theta_m^*}) \right|_2 \right] \\ &\leq \frac{c \hat{c} \tilde{c}}{\mu} \mathbb{E}_{\mathbb{P} \times \tilde{\mathbb{P}}} \left[\mathbf{1}_{\{n \geq k\}} \frac{1}{n} \left| M_{t_k} \odot (\hat{X}_{t_k-} - Y_{t_k-}^{\theta_m^*}) \right|_2^2 \right]^{1/2} \\ &\leq \frac{c \hat{c} \tilde{c}}{\mu} \mathbb{E}_{\mathbb{P} \times \tilde{\mathbb{P}}} \left[\mathbf{1}_{\{n \geq k\}} \frac{1}{n} \sum_{i=1}^n \left| M_{t_i} \odot (\hat{X}_{t_i-} - Y_{t_i-}^{\theta_m^*}) \right|_2^2 \right]^{1/2} \\ &\leq \frac{c \hat{c} \tilde{c}}{\mu} \mathbb{E}_{\mathbb{P} \times \tilde{\mathbb{P}}} \left[\frac{1}{n} \sum_{i=1}^n \left| M_{t_i} \odot (\hat{X}_{t_i-} - Y_{t_i-}^{\theta_m^*}) \right|_2^2 \right]^{1/2} \\ &\leq \frac{c \hat{c} \tilde{c}}{\mu} \left(\Phi(\theta_m^*) - \Psi(\hat{X}) \right)^{1/2} \xrightarrow{M \rightarrow \infty} 0, \end{aligned}$$

where we used first (10), (13) and (12) followed by two simply upper bounds and (11) in the last step. The same argument can be applied to show that $\lim_{m \rightarrow \infty} Y^{\theta_m^{\min}} = \hat{X}$ as a \mathbb{L} -limit. In particular, this proves that the limit $Y := \lim_{m \rightarrow \infty} Y^{\theta_m^{\min}}$ exists as \mathbb{L} -limit and by (Herrera et al., 2021, Lemma E.6) it equals \hat{X} ($\mathbb{P} \times \lambda_k$)-almost surely, for any $k \leq K$. \square

4.2 CONVERGENCE OF THE MONTE CARLO APPROXIMATION

We now assume the size m of the neural network and of the signature truncation level is fixed and we study the convergence of the Monte Carlo approximation when the number of samples N increases. Moreover, we show that both types of convergence can be combined. As in Herrera et al. (2021), we define $\tilde{\Theta}_M := \{\theta \in \Theta_M \mid |\theta|_2 \leq M\}$, which is a compact subspace of Θ_M a recall, that Θ_M in Theorem 4.1 can be replaced by $\tilde{\Theta}_M$. The convergence analysis is based on (Lapeyre & Lelong, 2021, Chapter 4.3) and follows (Herrera et al., 2021, Theorem E.13).

Theorem 4.3. *Let $\theta_{m,N}^{\min} \in \Theta_{m,N}^{\min} := \arg \inf_{\theta \in \tilde{\Theta}_m} \{\hat{\Phi}_N(\theta)\}$ for every $m, N \in \mathbb{N}$. Then, for every $m \in \mathbb{N}$, ($\mathbb{P} \times \tilde{\mathbb{P}}$)-a.s.*

$$\hat{\Phi}_N \xrightarrow{N \rightarrow \infty} \Phi \quad \text{uniformly on } \tilde{\Theta}_m.$$

Moreover, for every $m \in \mathbb{N}$, ($\mathbb{P} \times \tilde{\mathbb{P}}$)-a.s.

$$\Phi(\theta_{m,N}^{\min}) \xrightarrow{N \rightarrow \infty} \Phi(\theta_m^{\min}) \quad \text{and} \quad \hat{\Phi}_N(\theta_{m,N}^{\min}) \xrightarrow{N \rightarrow \infty} \Phi(\theta_m^{\min}).$$

In particular, one can define an increasing sequence $(N_m)_{m \in \mathbb{N}}$ in \mathbb{N} such that for every $1 \leq k \leq K$ we have that $Y^{\theta_{m, N_m}^{\min}}$ converges to \hat{X} for $m \rightarrow \infty$ as a random variable in $L^1(\Omega \times [0, T], \mathbb{P} \times \lambda_k)$. In particular, the limit process $Y := \lim_{m \rightarrow \infty} Y^{\theta_{m, N_m}^{\min}}$ equals \hat{X} $(\mathbb{P} \times \lambda_k)$ -almost surely as a random variable on $\Omega \times [0, T]$.

We define the separable Banach space $\mathcal{S} := \{x = (x_i)_{i \in \mathbb{N}} \in \ell^1(\mathbb{R}^d) \mid \|x\|_{\ell^1} < \infty\}$ for a suitable d (see below) with the norm $\|x\|_{\ell^1} := \sum_{i \in \mathbb{N}} |x_i|_2$, the function

$$F(x, y, z, m) := |m \odot (x - y)|_2 + |m \odot (y - z)|_2$$

and $\xi_j := (\xi_{j,0}, \dots, \xi_{j,n^j}, 0, \dots)$, where $\xi_{j,k} = (t_k^j, X_{t_k^j}^j, M_{t_k^j}^j, \pi_m(\tilde{X}^{\leq t_k^j, j})) \in \mathbb{R}^d$ and $t_k^j, M_{t_k^j}^j$ and $X_{t_k^j}^j$ (with 0 entries for coordinates which are not observed) are random variables describing the j -th realization of the training data, as defined in Section 3.3.1. Let $n^j(\xi_j) := \max_{k \in \mathbb{N}} \{\xi_{j,k} \neq 0\}$, $t_k(\xi_j) := t_k^j$, $X_k(\xi_j) := X_{t_k^j}^j$ and $M_k(\xi_j) := M_{t_k^j}^j$. By this definition we have $n^j = n^j(\xi_j)$ $(\mathbb{P} \times \tilde{\mathbb{P}})$ -almost-surely. Moreover, we have that ξ_j are i.i.d. random variables taking values in \mathcal{S} . Let us write $Y_t^\theta(\xi)$ to make the dependence of Y on the input and the weight θ explicit. Then we define

$$h(\theta, \xi_j) := \frac{1}{n^j(\xi_j)} \sum_{i=1}^{n^j(\xi_j)} F\left(X_i(\xi_j), Y_{t_i(\xi_j)}^\theta(\xi_j), Y_{t_i(\xi_j)-}^\theta(\xi_j), M_i(\xi_j)\right)^2.$$

Lemma 4.4. *Almost-surely the random function $\theta \in \tilde{\Theta}_M \mapsto Y_t^\theta$ is uniformly continuous for every $t \in [0, T]$.*

Proof. Since the activation functions of the neural networks can be assumed to be continuous, also the neural networks are continuous with respect to their weights θ , which implies that also $\theta \in \tilde{\Theta}_M \mapsto Y_t^\theta$ is continuous. Since $\tilde{\Theta}_M$ is compact, this automatically yields uniform continuity. \square

Proof of Theorem 4.3. First we note that, Y_t^θ is the (integration over the) output of neural networks and therefore bounded in terms of the input, the weights (which are bounded by m), T and some constant depending on the architecture and the activation functions of the neural network. In particular we have that $|Y_t^\theta(\xi_j)| \leq B(1 + X^{*,j})^p$ for all $t \in [0, T]$ and $\theta \in \tilde{\Theta}_m$ for some constant B , where $X^{*,j}$ corresponds to the input ξ_j . Hence,

$$\begin{aligned} & F\left(X_i(\xi_j), Y_{t_i(\xi_j)}^\theta(\xi_j), Y_{t_i(\xi_j)-}^\theta(\xi_j), M_i(\xi_j)\right)^2 \\ &= \left(\left| M_i(\xi_j) \odot (X_i(\xi_j) - Y_{t_i(\xi_j)}^\theta(\xi_j)) \right|_2 + \left| M_i(\xi_j) \odot (Y_{t_i(\xi_j)}^\theta(\xi_j) - Y_{t_i(\xi_j)-}^\theta(\xi_j)) \right|_2 \right)^2 \\ &\leq (4B(1 + X^{*,j})^p)^2 = 16B^2(1 + X^{*,j})^{2p}. \end{aligned}$$

Hence,

$$\mathbb{E}_{\mathbb{P} \times \tilde{\mathbb{P}}} \left[\sup_{\theta \in \tilde{\Theta}_M} h(\theta, \xi_j) \right] \leq \mathbb{E}_{\mathbb{P} \times \tilde{\mathbb{P}}} \left[\frac{1}{n} \sum_{i=1}^n 16B^2(1 + X^{*,j})^{2p} \right] < \infty, \quad (14)$$

by Assumption 2.1. By Lemma 4.4, the function $\theta \mapsto h(\theta, \xi_1)$ is continuous, hence, we can apply (Herrera et al., 2021, Lemma E.15), yielding that almost-surely for $N \rightarrow \infty$ the function

$$\theta \mapsto \frac{1}{N} \sum_{j=1}^N h(\theta, \xi_j) = \hat{\Phi}_N(\theta) \quad (15)$$

converges uniformly on $\tilde{\Theta}_m$ to

$$\theta \mapsto \mathbb{E}_{\mathbb{P} \times \tilde{\mathbb{P}}} [h(\theta, \xi_1)] = \Phi(\theta). \quad (16)$$

We deduce from (Herrera et al., 2021, Lemma E.14) that $d(\theta_{m, N}^{\min}, \Theta_m^{\min}) \rightarrow 0$ a.s. when $N \rightarrow \infty$. Then there exists a sequence $(\hat{\theta}_{m, N}^{\min})_{N \in \mathbb{N}}$ in Θ_m^{\min} such that $|\theta_{m, N}^{\min} - \hat{\theta}_{m, N}^{\min}|_2 \rightarrow 0$ a.s. for $N \rightarrow \infty$. The uniform continuity of the random functions $\theta \mapsto Y_t^\theta$ on $\tilde{\Theta}_m$ implies that

$$|Y_t^{\theta_{m, N}^{\min}}(\xi_1) - Y_t^{\hat{\theta}_{m, N}^{\min}}(\xi_1)|_2 \rightarrow 0 \text{ a.s. for all } t \in [0, T] \text{ as } N \rightarrow \infty.$$

By continuity of F this yields $|h(\theta_{m,N}^{\min}, \xi_1) - h(\hat{\theta}_{m,N}^{\min}, \xi_1)| \rightarrow 0$ a.s. as $N \rightarrow \infty$. With (14) we can apply dominated convergence which yields

$$\lim_{N \rightarrow \infty} \mathbb{E}_{\mathbb{P} \times \tilde{\mathbb{P}}} \left[|h(\theta_{m,N}^{\min}, \xi_1) - h(\hat{\theta}_{m,N}^{\min}, \xi_1)| \right] = 0.$$

Since for every integrable random variable Z we have $0 \leq |\mathbb{E}[Z]| \leq \mathbb{E}[|Z|]$ and since $\hat{\theta}_{m,N}^{\min} \in \Theta_m^{\min}$ we can deduce

$$\lim_{N \rightarrow \infty} \Phi(\theta_{m,N}^{\min}) = \lim_{N \rightarrow \infty} \mathbb{E}_{\mathbb{P} \times \tilde{\mathbb{P}}} [h(\theta_{m,N}^{\min}, \xi_1)] = \lim_{N \rightarrow \infty} \mathbb{E}_{\mathbb{P} \times \tilde{\mathbb{P}}} [h(\hat{\theta}_{m,N}^{\min}, \xi_1)] = \Phi(\theta_m^{\min}). \quad (17)$$

Now by triangle inequality,

$$|\hat{\Phi}_N(\theta_{m,N}^{\min}) - \Phi(\theta_m^{\min})| \leq |\hat{\Phi}_N(\theta_{m,N}^{\min}) - \Phi(\theta_{m,N}^{\min})| + |\Phi(\theta_{m,N}^{\min}) - \Phi(\theta_m^{\min})|. \quad (18)$$

(15), (16) and (17) imply that both terms on the right hand side converge to 0 when $N \rightarrow \infty$, which finishes the proof of the first part of the Theorem.

We define $N_0 := 0$ and for every $m \in \mathbb{N}$

$$N_m := \min \left\{ N \in \mathbb{N} \mid N > N_{m-1}, |\Phi(\theta_{m,N}^{\min}) - \Phi(\theta_m^{\min})| \leq \frac{1}{m} \right\},$$

which is possibly due to (17). Then Theorem 4.1 implies that

$$|\Phi(\theta_{m,N_m}^{\min}) - \Psi(\hat{X})| \leq \frac{1}{m} + |\Phi(\theta_m^{\min}) - \Psi(\hat{X})| \xrightarrow{m \rightarrow \infty} 0.$$

Therefore, we can apply the same arguments as in the proof of Theorem 4.1 (starting from (11)) to show that

$$\mathbb{E}_{\mathbb{P} \times \lambda_k} \left[\left| \hat{X} - Y^{\theta_{m,N_m}^{\min}} \right|_2 \right] \leq \frac{c \hat{c} \tilde{c}}{\mu} \left(\Phi(\theta_{m,N_m}^{\min}) - \Psi(\hat{X}) \right)^{1/2} \xrightarrow{m \rightarrow \infty} 0,$$

for every $1 \leq k \leq K$. □

Corollary 4.5. *In the setting of Theorem 4.3, we also have that $(\mathbb{P} \times \tilde{\mathbb{P}})$ -a.s.*

$$\Phi(\theta_{m,N_m}^{\min}) \xrightarrow{m \rightarrow \infty} \Psi(\hat{X}) \quad \text{and} \quad \hat{\Phi}_{\tilde{N}_m}(\theta_{m,\tilde{N}_m}^{\min}) \xrightarrow{m \rightarrow \infty} \Psi(\hat{X}),$$

where $(\tilde{N}_m)_{m \in \mathbb{N}}$ is another increasing sequence in \mathbb{N} .

Proof. The first convergence result was already shown in the proof of Theorem 4.3 and the second one can be shown similarly, when defining \tilde{N}_m by $\tilde{N}_0 := 0$ and for every $m \in \mathbb{N}$

$$\tilde{N}_m := \min \left\{ N \in \mathbb{N} \mid N > \tilde{N}_{m-1}, |\hat{\Phi}_N(\theta_{m,N}^{\min}) - \Phi(\theta_m^{\min})| \leq \frac{1}{m} \right\},$$

which is possibly due to (18). □

Remark 4.6. *Theorem 4.1, Theorem 4.3 and Corollary 4.5 hold equivalently, when replacing the terms $(Z_{t_i} - Z_{t_i-})$ and $\left(Y_{t_i^{(j)}}^{\theta,j} - Y_{t_i^{(j)}-}^{\theta,j} \right)$ in (6), (7) and (8), by $(X_{t_i} - Z_{t_i-})$ and $\left(X_{t_i^{(j)}}^{(j)} - Y_{t_i^{(j)}-}^{\theta,j} \right)$ respectively. We will refer to this adjustment as of the objective function as equivalent objective (or loss) function.*

4.3 OVERCOMING THE INDEPENDENCE OF THE UNDERLYING PROCESS AND ITS OBSERVATION TIMES

So far we have concentrated on the case where the observation times are independent of the underlying process. This was modelled by using the product space of two independent probability spaces. The main advantage of this approach is, that while this still allows for a quite high generality, it keeps the derivations of the results relatively easy, since the tool of splitting up into the components of the one and the other probability space can be used. This was done at several points to keep the argumentations easy.

Remark 4.7. *The same theoretical results can be derived in the general case where everything is defined on one probability space and no independence assumptions are imposed under mild constraints.*

We do not prove this remark here, but we give an intuitive explanation by the following example. If the observation times are given through a counting process with intensity $(\lambda(t))_{t \in [0, T]}$, where $\lambda(t)$ depends on X_t , then the assumption that there exists some $\epsilon > 0$ such that $\lambda(t) \geq \epsilon$ for all t is enough for PD-NJ-ODE to learn the conditional expectation⁵. Indeed, if the intensity was simply given by $\lambda(t) = \epsilon$ then our results hold and the PD-NJ-ODE output converges to the true conditional expectation. However, having an intensity higher than ϵ means that the probability of making an observation is larger, leading to more observations at this time, which can only lead to better predictions.

5 CONDITIONAL VARIANCE, MOMENTS AND MOMENT GENERATING FUNCTION

5.1 UNCERTAINTY ESTIMATION: CONDITIONAL VARIANCE

Let X be a d_X -dimensional process satisfying Assumption 2.1. If X^2 satisfies 4. & 5. of Assumption 2.1, then also the joint process $Z := (Z_1, Z_2) := (X, X^2)^\top$ satisfies Assumption 2.1. Therefore, the conditional expectation of Z can be used to get an uncertainty estimate for the prediction of the process X (not to be confused with an uncertainty estimate of our model output) by computing its conditional variance

$$\text{Var}[X_t | \mathcal{A}_{\tau(t)}] = \mathbb{E}[X_t^2 | \mathcal{A}_{\tau(t)}] - \mathbb{E}[X_t | \mathcal{A}_{\tau(t)}]^2 = \mathbb{E}[(Z_2)_t | \mathcal{A}_{\tau(t)}] - \mathbb{E}[(Z_1)_t | \mathcal{A}_{\tau(t)}]^2. \quad (19)$$

In particular, when using the $2d_X$ -dimensional input Z for NJ-ODE (where the observation mask is the same for Z_1 and Z_2), (19) yields a way to compute the conditional variance of X .

An example of a process X for which also its conditional variance can be estimated in our framework is given below.

Example 5.1 (Brownian Motion and its Conditional Variance). *If X is a standard Brownian motion and $Z := (X, X^2)^\top$ then we have that $\mathbb{E}[(Z_T^*)^p] < \infty$ for every $1 \leq p < \infty$ (compare with Section 6.6) and since $\text{Var}[X_{t+s} | X_t] = \text{Var}[X_{t+s} - X_t] = s$ we get*

$$\mathbb{E}[Z_t | \mathcal{A}_{\tau(t)}] = (X_{\tau(t)}, X_{\tau(t)}^2 + (t - \tau(t)))^\top = ((Z_1)_{\tau(t)}, (Z_2)_{\tau(t)} + (t - \tau(t)))^\top.$$

Hence, $f_1(s, \tau(t), \tilde{X}^{\leq \tau(t)}) = 0$ and $f_2(s, \tau(t), \tilde{X}^{\leq \tau(t)}) = 1$ and therefore Assumption 2.1 is satisfied for Z .

5.2 TOWARDS THE CONDITIONAL DISTRIBUTION: MOMENTS AND THE MOMENT GENERATING FUNCTION

In the following we assume for simplicity that the process X is 1-dimensional, although the considerations generalize to higher dimensions. If the process X is such that all its moments X^n for $n \in \mathbb{N}$ satisfy Assumption 2.1, then, in principle, NJ-ODE can be used to compute all conditional moments of X . Theorem 3.3.11 and the Remark afterwards of (Durrett, 2010) give two conditions on the moments under which they uniquely characterize the corresponding distribution. Hence, if one of these conditions is satisfied, NJ-ODE can, in principle, characterize the conditional distribution of X_t given $\mathcal{A}_{\tau(t)}$ for any $t \in [0, T]$.

Under the stronger assumption, that there exists some $\delta > 0$ such that for all $u \in (-\delta, \delta)$ the process $\exp(uX)$ satisfies Assumption 2.1, NJ-ODE can in principle be used to compute the conditional moment function of X , $\hat{m}_X(u)_t := \mathbb{E}[\exp(uX_t) | \mathcal{A}_{\tau(t)}]$ for $u \in (-\delta, \delta)$, for any $t \in [0, T]$. Since the moment generating function on any open interval including 0 uniquely characterizes the corresponding distribution (Billingsley, 1995, Sec. 30), NJ-ODE then, in principle, characterizes the conditional distribution.

In practice, only finitely many moments can be computed and the moment generating function can only be approximated by computing it for finitely many values of u . However, the two methods described above give rise to a way how NJ-ODE can approximately characterize the conditional distribution of X .

⁵An example of such an intensity would be $\lambda(t) := \epsilon + |X_t|$.

6 EXAMPLES OF PROCESSES SATISFYING THE ASSUMPTIONS

We summarise several processes that satisfy Assumption 2.1. The examples in Sections 6.1 and 6.2 are from (Herrera et al., 2021) and recalled here, to show that the new setting truly is a generalization of the old one. In Section 6.4 we present a process with jumps, in Sections 6.5 and 6.3 path-dependent processes and in Section 6.6 a multivariate process with incomplete observations.

6.1 ITÔ DIFFUSION WITH REGULARITY ASSUMPTIONS

Let $\{W_t\}_{t \in [0, T]}$ be an d_W -dimensional Brownian motion on $(\Omega, \mathcal{F}, \mathbb{F} := \{\mathcal{F}_t\}_{0 \leq t \leq T}, \mathbb{P})$, for $d_W \in \mathbb{N}$. Let $X := (X_t)_{t \in [0, T]}$ be defined as the solution of the stochastic differential equation (SDE)

$$dX_t = \mu(t, X_t)dt + \sigma(t, X_t)dW_t, \quad (20)$$

for all $0 \leq t \leq T$, where $X_0 = x \in \mathbb{R}^{d_x}$ is the starting point and the measurable functions $\mu : [0, T] \times \mathbb{R}^{d_x} \rightarrow \mathbb{R}^{d_x}$ and $\sigma : [0, T] \times \mathbb{R}^{d_x} \rightarrow \mathbb{R}^{d_x \times d_W}$ are the *drift* and the *diffusion* respectively. By definition this process is continuous. Moreover, we impose the following assumptions:

- **μ and σ are both globally Lipschitz continuous in their second component**, i.e. for $\varphi \in \{\mu, \sigma\}$ there exists a constant $\tilde{M} > 0$ such that for all $t \in [0, T]$

$$|\varphi(t, x) - \varphi(t, y)|_2 \leq \tilde{M}|x - y|_2 \quad \text{and} \quad |\varphi(t, x)|_2 \leq (1 + |x|_2)\tilde{M}.$$

In particular, their growth is at most linear in the second component.

- **μ is bounded, and continuous in its first component (t) uniformly in its second component (x)**, i.e. for every $t \in [0, T]$ and $\varepsilon > 0$ there exists a $\delta > 0$ such that for all $s \in [0, T]$ with $|t - s| < \delta$ and all $x \in \mathbb{R}^{d_x}$ we have $|\mu(t, x) - \mu(s, x)| < \varepsilon$.
- **σ is càdlàg (right-continuous with existing left-limit) in the first component and L^2 integrable with respect to W** , $\sigma \in L^2(W)$, i.e.

$$\mathbb{E} \left[\sum_{i=1}^{d_x} \sum_{j=1}^{d_W} \int_0^T \sup_x \sigma_{i,j}(x, t)^2 d[W^j, W^j]_t \right] = \int_0^T \sup_x |\sigma(x, t)|_F^2 dt < \infty, \quad (21)$$

where $|\cdot|_F$ denotes the Frobenius matrix norm. This is in particular implied if σ is bounded.

- We always observe all coordinates of X simultaneously (i.e. no incomplete observations).

Remark 6.1. In (Herrera et al., 2021) there was the additional assumption that X is continuous and square integrable, which we left out here, since this is always implied through the other assumptions.

Under these assumptions a unique continuous solution of (20) exists, once an initial value is fixed (Protter, 2005, Thm. 7, Chap. V). (Herrera et al., 2021, Lemma E.7) shows that X^* is L^2 -integrable. Moreover, the results (Herrera et al., 2021, Propositions B.1 and B.4) imply that Assumption 2.1 is satisfied.

Remark 6.2. The assumption that μ is bounded and the integrability assumption on σ can be weakened, as will be shown in Section 6.3. In particular, the boundedness of μ is only needed to apply the Markov property, which is not needed in our more general setting now, where we have access to the entire past information.

6.2 OTHER ITÔ DIFFUSIONS: BLACK-SCHOLES, ORNSTEIN-UHLENBECK, HESTON

The Black-Scholes (geometric Brownian Motion), Ornstein-Uhlenbeck and Heston processes are Itô diffusions which do not satisfy the assumptions in Section 6.1. In particular, their drifts are not bounded and the Heston process does not satisfy the Lipschitz assumptions. If the Feller condition is satisfied, the Heston process is Lipschitz with high probability, otherwise not. Nevertheless, Assumption 2.1 is still satisfied for these three processes as shown below. Experiments on these processes were performed in (Herrera et al., 2021).

Example 6.3 (Black-Scholes). *The SDE describing this model is*

$$dX_t = \mu X_t dt + \sigma X_t dW_t, \quad X_0 = x_0,$$

where W is a 1-dimensional Brownian motion and $\mu, \sigma \geq 0$. The conditional expectation of the solution process X is given by $\hat{X}_t = E(X_t | X_{\tau(t)}) = X_{\tau(t)} e^{\mu(t-\tau(t))}$. Hence, $f(s, \tau(t), \tilde{X}^{\leq \tau(t)}) = X_{\tau(t)} \mu e^{\mu(s-\tau(t))}$.

(Cohen & Elliott, 2015, Lemma 16.1.4) implies that $\mathbb{E}[(X_T^*)^p] < \infty$ for every $2 \leq p < \infty$ and therefore by Hölder's inequality for all $1 \leq p < \infty$.

Example 6.4 (Ornstein-Uhlenbeck). This model is described by the SDE

$$dX_t = -k(X_t - m)dt + \sigma dW_t, \quad X_0 = x_0,$$

where W is a 1-dimensional Brownian motion and $k, m, \sigma > 0$. The conditional expectation of the solution process X is given by $\hat{X}_t = E(X_t | X_{\tau(t)}) = X_{\tau(t)} e^{-k(t-\tau(t))} + m(1 - e^{-k(t-\tau(t))})$. Hence, $f(s, \tau(t), \tilde{X}^{\leq \tau(t)}) = -X_{\tau(t)} k e^{-k(s-\tau(t))} + m k e^{-k(s-\tau(t))}$.

Again (Cohen & Elliott, 2015, Lemma 16.1.4) implies that $\mathbb{E}[(X_T^*)^p] < \infty$ for every $2 \leq p < \infty$ and therefore by Hölder's inequality for all $1 \leq p < \infty$.

Example 6.5 (Heston). The Heston model is described by the SDE

$$\begin{aligned} dX_t &= \mu X_t dt + \sqrt{v_t} X_t dW_t \\ dv_t &= -k(v_t - m)dt + \sigma \sqrt{v_t} dB_t \end{aligned}$$

where W and B are 1-dimensional Brownian motions with correlation $\rho \in (-1, 1)$, $\mu \geq 0$ and $k, m, \sigma > 0$. The conditional expectation of the solution process X is given by $\hat{X}_t = E(X_t | X_{\tau(t)}) = X_{\tau(t)} e^{\mu(t-\tau(t))}$. Hence, $f_1(s, \tau(t), \tilde{X}^{\leq \tau(t)}) = X_{\tau(t)} \mu e^{\mu(s-\tau(t))}$. Moreover, if also the stochastic variance should be predicted coincidentally, its conditional expectation is given by $\hat{v}_t = E(v_t | v_{\tau(t)}) = v_{\tau(t)} e^{-k(t-\tau(t))} + m(1 - e^{-k(t-\tau(t))})$. Hence, $f_2(s, \tau(t), \tilde{v}^{\leq \tau(t)}) = -v_{\tau(t)} k e^{-k(s-\tau(t))} + m k e^{-k(s-\tau(t))}$.

L^p -integrability of the Heston model is more delicate. While (Cohen & Elliott, 2015, Lemma 16.1.4) implies that $\mathbb{E}[(v_T^*)^p] < \infty$ for every $2 \leq p < \infty$ and therefore by Hölder's inequality for all $1 \leq p < \infty$, the moments of X can explode (Andersen & Piterberg, 2007, Proposition 3.1). In particular, the moment explosion time

$$T_*(p) := \sup\{t \geq 0 \mid \mathbb{E}[|X_t|^p] < \infty\}$$

of X is infinite if and only if $\rho\sigma p < k$ and $(\rho\sigma p - k)^2 - \sigma^2(p^2 - p) \geq 0$. By Itô's lemma we can write $X_t = \exp(\mu t + Z_t)$, where Z_t is the discounted log-price process satisfying

$$dZ_t = -\frac{v_t}{2} dt + \sqrt{v_t} dW_t.$$

According to (Keller-Ressel, 2011, Corollary 2.7 and Equation 6.1), $\exp(Z_t)$ is a martingale, hence Doob's Maximal inequality implies that for any $1 < p < \infty$

$$\mathbb{E}[(X_T^*)^p] \leq \frac{p}{p-1} \exp(\mu T) \mathbb{E}[|X_T|^p].$$

Therefore, X_T^* is L^p -integrable if $T < T_*(p)$, where a closed form for $T_*(p)$ is given in (Andersen & Piterberg, 2007, Proposition 3.1), in case it is finite. Again, Hölder's inequality implies that X_T^* is L^1 -integrable if it is L^p -integrable for some $p > 1$.

Remark 6.6. $T_*(p) = \infty$ if

$$p < \min \left(\frac{k}{\rho\sigma}, \frac{(\sigma^2 - 2k\sigma\rho) + \sqrt{(\sigma^2 - 2k\sigma\rho)^2 + 4\sigma^2(1 - \rho^2)k^2}}{2\sigma^2(1 - \rho^2)} \right).$$

Note that $(1 - \rho^2) > 0$, therefore the second term is an element of \mathbb{R}_+ .

In the standard Heston example of (Herrera et al., 2021), the used parameters are $\mu = 2$, $\sigma = 0.3$, $k = 2$, $m = 4$, $\rho = 0.5$ and therefore $T_*(p) = \infty$ for all $p \leq 4.7972$. In the second example of (Herrera et al., 2021) of a Heston model where the Feller condition is not satisfied, the used parameters are $\mu = 2$, $\sigma = 3$, $k = 2$, $m = 1$, $\rho = 0.5$ and therefore $T_*(p) = \infty$ for all $p \leq 1.0234\dots$. Moreover, for $p = 2$ we have $T_*(2) > 0.6465$.

6.3 STOCHASTIC FUNCTIONAL DIFFERENTIAL EQUATIONS

Following the definitions in Section 16.2 of (Cohen & Elliott, 2015), let \mathcal{D} be the space of càdlàg adapted processes on \mathbb{R}_X^d and $S^p \subset \mathcal{D}$ for $1 \leq p < \infty$, the set of all processes $X \in \mathcal{D}$ for which

$$\|X\|_{S^p} := \|X_T^*\|_{L^p} = \mathbb{E}[(X_T^*)^p]^{1/p}$$

where $X^* = \max_i \{X_i^*\}$ for multidimensional processes and where we use the finite time horizon T instead of ∞ . We look at functions $f : \Omega \times [0, T] \times \mathcal{D} \rightarrow \mathbb{R}^{u \times v}$, $(\omega, t, X) \mapsto f(\omega, t, X) = f(X)$ that are uniformly Lipschitz, i.e., there exists some $L \in \mathbb{R}$ such that for any $X, Y \in \mathcal{D}$ and $t \in [0, T]$,

$$(f(X) - f(Y))_t^* \leq L(X - Y)_{t-}^*. \quad (22)$$

For such functions we write $f \in \text{Lip}(L)$. It is clear from this definition, that $f(X)_t$ only depends on $(X_s)_{0 \leq s \leq t}$. Moreover, for such functions we have that $\|f(X) - f(Y)\|_{S^p} \leq L\|X - Y\|_{S^p}$.

Let $2 \leq p < \infty$, $d_W \in \mathbb{N}$ and let $(W_t)_{t \in [0, T]}$ be a d_W -dimensional Brownian motion on the probability space $(\Omega, \mathcal{F}, \mathbb{P} := (\mathcal{F}_t)_{0 \leq t \leq T}, \mathbb{P})$. We assume that the stochastic process $X := (X_t)_{t \in [0, T]}$ is defined as the continuous solution of the stochastic functional differential equation

$$dX_t = \mu(\omega, t, X) dt + \sigma(\omega, t, X) dW_t, = \mu(X)_t dt + \sigma(X)_t dW_t \quad (23)$$

for all $0 \leq t \leq T$ with (random) starting point X_0 taking values in \mathbb{R}^{d_X} such that $\|X_0\|_{L^p} < \infty$, drift function $\mu : \Omega \times [0, T] \times \mathcal{D} \rightarrow \mathbb{R}^{d_X}$ and diffusion function $\sigma : \Omega \times [0, T] \times \mathcal{D} \rightarrow \mathbb{R}^{d_X \times d_W}$. We assume that μ and σ are uniformly Lipschitz in the sense of (22) and that there exists a constant $C > L$ such that $\|\mu(0)\|_{S^p} + \|\sigma(0)\|_{S^p} < C$. Moreover, we assume that we always observe all coordinates of X simultaneously. These assumptions imply that μ and σ have linear growth,

$$\begin{aligned} \|\mu(X)\|_{S^p} &= \|\mu(0)\|_{S^p} + (\|\mu(X)\|_{S^p} - \|\mu(0)\|_{S^p}) \leq \|\mu(0)\|_{S^p} + \|\mu(X)^* - \mu(0)^*\|_{L^p} \\ &\leq \|\mu(0)\|_{S^p} + \|\mu(X) - \mu(0)\|_{S^p} \leq \|\mu(0)\|_{S^p} + L\|X\|_{S^p} \leq C(1 + \|X\|_{S^p}), \end{aligned}$$

and similar for σ .

It is easy to see that $(W_t)_{0 \leq t \leq T}$ and $(t)_{0 \leq t \leq T}$ are both α -sliceable for any $\alpha > 0$ (Cohen & Elliott, 2015, Definition 16.3.8), in fact even with deterministic stopping times. Therefore, (Cohen & Elliott, 2015, Lemma 16.3.10) implies that there exists a unique solution to (23) and that this solution satisfies

$$\|X\|_{S^p} \leq \tilde{C}(\|X_0\|_{L^p} + \|\mu(0)\|_{S^p} + \|\sigma(0)\|_{S^p}),$$

for some \tilde{C} depending only on L and W . In particular, we can choose C such that $\|X\|_{S^p} < C$. This implies integrability of the drift and diffusion component

$$\begin{aligned} \mathbb{E} \left[\int_0^T |\mu(X)_t| + |\sigma(X)_t| dt \right] &= \int_0^T \mathbb{E} [|\mu(X)_t| + |\sigma(X)_t|] dt \\ &\leq \int_0^T (\|\mu(X)\|_{S^p} + \|\sigma(X)\|_{S^p}) dt \\ &\leq 2TC(1 + C), \end{aligned} \quad (24)$$

where we used Fubini's Theorem in the first step.

(24) yields that the process

$$\tilde{M}_t := \int_0^t \sigma(s, X_s, X_{<s}) dW_s, \quad 0 \leq t \leq T,$$

is a square integrable martingale (Protter, 2005, Lemma before Thm. 28, Chap. IV) since the Brownian motion W is square integrable with $d[W^i, W^j]_t = \delta_{i,j} dt$. Using the martingale property of \tilde{M} and the tower property for $\mathcal{A}_{\tau(t)} \subset \mathcal{F}_{\tau(t)}$, we have ($\tilde{\omega}$ -wise) for every $t \in [0, T]$,

$$\begin{aligned} \hat{X}_t &= \mathbb{E}_{\mathbb{P}} [(X_t - X_{\tau(t)}) + X_{\tau(t)} | \mathcal{A}_{\tau(t)}] \\ &= X_{\tau(t)} + \mathbb{E}_{\mathbb{P}} \left[\int_{\tau(t)}^t \mu(X)_r dr | \mathcal{A}_{\tau(t)} \right] + \mathbb{E}_{\mathbb{P}} \left[\int_{\tau(t)}^t \sigma(X)_r dW_r | \mathcal{A}_{\tau(t)} \right] \\ &= X_{\tau(t)} + \int_{\tau(t)}^t \mathbb{E}_{\mathbb{P}} [\mu(X)_r | \mathcal{A}_{\tau(t)}] dr + \mathbb{E}_{\mathbb{P}} [\mathbb{E}_{\mathbb{P}} [M_t - M_{\tau(t)} | \mathcal{F}_{\tau(t)}] | \mathcal{A}_{\tau(t)}] \\ &= X_{\tau(t)} + \int_{\tau(t)}^t \mathbb{E}_{\mathbb{P}} [\mu(X)_r | \mathcal{A}_{\tau(t)}] dr, \end{aligned} \quad (25)$$

where we used Fubini's theorem (for conditional expectation) in the second last step, which is justified because of (24). Let us define $\Delta := \{(t, r) \in [0, T]^2 | t + r \leq T\}$ and the function

$$\begin{aligned} \tilde{\mu} : \Delta \times BV([0, T]) &\rightarrow \mathbb{R}^{d \times d} \\ ((t, r), \xi) &\mapsto \mathbb{E}_{\mathbb{P}} \left[\mu(\omega, t + r, X) | \tilde{X}^{\leq t} = \xi \right], \end{aligned}$$

then the Doob-Dynkin Lemma (Taraldsen, 2018, Lemma 2) implies that we can rewrite (25) as

$$\hat{X}_t = X_{\tau(t)} + \int_{\tau(t)}^t \tilde{\mu} \left(\tau(t), r - \tau(t), \tilde{X}^{\leq \tau(t)} \right) dr. \quad (26)$$

To satisfy Assumption 2.1, we need that $\tilde{\mu}$ is continuous. While this might not be true in general, the following examples give cases where this can be shown.

Example 6.7. Under the additional assumption that μ and σ only depend on the current value of X and not its entire path, (Gubinelli, 2016, Theorem 8) together with (Herrera et al., 2021, Proposition B.4) prove that $\tilde{\mu}$ is continuous. Importantly, here we do not need the boundedness assumption for μ nor the integrability assumption for σ , hence this generalizes the example from Section 6.1 as described in Remark 6.2. Notice that by adding further factors to the state space of X , which are unobserved and which follow a Markovian dynamics satisfying mild regularity conditions, we can include many path dependence structures of the drift and therefore also obtain continuous dependence of $\tilde{\mu}$ (with respect to those factors) in an analogous manner.

Example 6.8. If we additionally assume that $\mu(X)_t = \alpha X_t + \beta$ for some $\alpha, \beta \in \mathbb{R}$, i.e. linear in the current value of X , while σ can be general and path dependent, we can show that $\tilde{\mu}$ is continuous. Indeed, then it follows from (25) that

$$\mathbb{E}_{\mathbb{P}} [X_t | \mathcal{A}_{\tau(t)}] = X_{\tau(t)} + \int_{\tau(t)}^t (\alpha \mathbb{E}_{\mathbb{P}} [X_r | \mathcal{A}_{\tau(t)}] + \beta) dr. \quad (27)$$

(27) is equivalent to the ordinary differential equation

$$\begin{aligned} y'(t) &= \alpha y(t) + \beta, \quad t \geq \tau(t), \\ y(\tau(t)) &= y_{\tau} := X_{\tau(t)}, \end{aligned}$$

by defining $y(r) := \mathbb{E}_{\mathbb{P}} [X_r | \mathcal{A}_{\tau(t)}]$ for $r \geq \tau(t)$. The unique solution to this initial value problem is given by $y(t) = -\frac{\beta}{\alpha} + \left(\frac{\beta}{\alpha} + y_{\tau}\right) e^{\alpha(t-\tau)}$ hence the conditional expectation between $\tau(t)$ and the next observation is given by

$$\mathbb{E}_{\mathbb{P}} [X_r | \mathcal{A}_{\tau(t)}] = F(r, \tau, \tilde{X}^{\leq \tau}) = -\frac{\beta}{\alpha} + \left(\frac{\beta}{\alpha} + X_{\tau(t)}\right) e^{\alpha(r-\tau)},$$

which is continuous and differentiable in t leading to

$$\tilde{\mu} \left(\tau, r - \tau, \tilde{X}^{\leq \tau} \right) = \alpha \mathbb{E}_{\mathbb{P}} [X_r | \mathcal{A}_{\tau}] + \beta = (\beta + \alpha X_{\tau}) e^{\alpha(r-\tau)} = f(r, \tau, \tilde{X}^{\leq \tau}) = \frac{\partial}{\partial r} F(r, \tau, \tilde{X}^{\leq \tau}).$$

6.4 STOCHASTIC PROCESS WITH JUMPS: HOMOGENEOUS POISSON POINT PROCESS

A homogeneous Poisson point process $(N_t^{\lambda})_{t \geq 0}$, for $\lambda > 0$, is defined to be the increasing stochastic process in $\mathbb{R}_{\geq 0}$ such that $N_0^{\lambda} = 0$ and its increments are independent Poisson distributed, i.e. $N_t^{\lambda} - N_s^{\lambda} \sim \text{Poisson}(\lambda(t-s))$ for any $0 \leq s \leq t$. It follows that its conditional expectation is $\hat{N}_t^{\lambda} = E(N_t^{\lambda} | \mathcal{N}_{\tau(t)}^{\lambda}) = E(N_{\tau(t)}^{\lambda} + (N_t^{\lambda} - N_{\tau(t)}^{\lambda}) | \mathcal{N}_{\tau(t)}^{\lambda}) = N_{\tau(t)}^{\lambda} + \lambda(t - \tau(t))$. Therefore, $f(s, \tau(t), \tilde{N}^{\lambda, \leq \tau(t)}) = \lambda$.

By its definition as an increasing process, $(N_T^{\lambda})_T^* = N_T^{\lambda}$, and since $N_T^{\lambda} \sim \text{Poisson}(\lambda(T))$ all moments exists, hence $\mathbb{E}[\left((N^{\lambda})_T^*\right)^p] < \infty$ for all $1 \leq p < \infty$.

6.5 FRACTIONAL BROWNIAN MOTION

Definition 6.9. A random vector $(X_1, \dots, X_n) \in \mathbb{R}^n$ is a centered Gaussian vector if any linear combination of the X_i is a centered Gaussian random variable.

Definition 6.10. A stochastic process $(X_t)_{t \in I}$ is a centered Gaussian process if any finite-dimensional vector $(X_{t_1}, \dots, X_{t_p})$ is a centered Gaussian vector.

Since the law of a centered Gaussian vector is completely determined by its covariance function, it suffices to specify the covariance to obtain a unique Gaussian process. In fact, one can prove that for each function $S : I \times I \rightarrow \mathbb{R}$ such that for all t_1, \dots, t_p in I and for all $\lambda_1, \dots, \lambda_p$ in \mathbb{R} ,

$$\sum_{1 \leq i, j \leq p} \lambda_i \lambda_j S(t_i, t_j) \geq 0,$$

we can construct a centered Gaussian process $(X_t)_{t \in I}$ with the given covariance function S , using Kolmogorov's extension theorem.

Definition 6.11. The fractional Brownian motion $B^H = (B_t^H)_{t \in \mathbb{R}_+}$ with Hurst index $H \in (0, 1]$ is the centered Gaussian process with covariance function

$$r_H(t, s) = \frac{1}{2} [t^{2H} + s^{2H} - |t - s|^{2H}].$$

Note that the case $H = \frac{1}{2}$ results in a covariance of $\frac{1}{2} [t + s - |t - s|] = \min(s, t)$, which is precisely the covariance of a standard Brownian motion. The case $H > \frac{1}{2}$ corresponds to positively correlated increments, which is a common phenomenon in financial mathematics. Meanwhile, the case $H < \frac{1}{2}$ corresponds to negatively correlated increments.

If $H \neq \frac{1}{2}$, the paths are non-Markovian, hence, the conditional expectation does not only include the information of the last measurement, as we have seen for the Black-Scholes, Heston and Ornstein-Uhlenbeck model. Instead, the conditional process (of which the mean is the conditional expectation) of the fractional Brownian motion depends on the entire past trajectory. In (Sottinen & Viitasaari, 2017, p. 3), the law of this conditional process is described explicitly. It requires knowledge of the whole trajectory of the fractional Brownian motion up to the current time. Since, in our setting, we only have a finite number of observations (at random times) available to train our model, it is unreasonable to expect the model to correctly approximate the conditional expectation implied by this conditional process. However, we can also compute the true conditional expectation given our discrete observations, making use of the fact that B^H is a Gaussian process, implying that the vector of observations is a Gaussian vector (Norros et al., 1999). Assume we have observed the values $(B_{t_1}^H, \dots, B_{t_\nu}^H)$ of B^H at times $0 < t_1 < \dots < t_\nu < T$ and we want to compute the conditional expectation $\mathbb{E}[B_t^H | (B_{t_1}^H, \dots, B_{t_\nu}^H)]$ for $t \geq t_\nu$. For any fixed t , the vector $(B_{t_1}^H, \dots, B_{t_\nu}^H, B_t^H)$ is centred Gaussian with covariance

$$R = \begin{pmatrix} r_H(t_1, t_1) & \dots & r_H(t_1, t) \\ \vdots & \ddots & \vdots \\ r_H(t_1, t) & \dots & r_H(t, t) \end{pmatrix} =: \begin{pmatrix} R_\nu & R_{\nu,1} \\ R_{1,\nu} & r_H(t, t) \end{pmatrix}.$$

Then a simple calculation shows that

$$\text{cov} (B_t^H - R_{1,\nu} R_\nu^{-1} (B_{t_1}^H, \dots, B_{t_\nu}^H)^\top, (B_{t_1}^H, \dots, B_{t_\nu}^H)) = R_{1,\nu} - R_{1,\nu} R_\nu^{-1} R_\nu = 0,$$

implying that $B_t^H - R_{1,\nu} R_\nu^{-1} (B_{t_1}^H, \dots, B_{t_\nu}^H)^\top$ is independent of $(B_{t_1}^H, \dots, B_{t_\nu}^H)$, since it is a Gaussian vector. Hence,

$$\begin{aligned} \mathbb{E} [B_t^H | (B_{t_1}^H, \dots, B_{t_\nu}^H)] &= \mathbb{E} [B_t^H - R_{1,\nu} R_\nu^{-1} (B_{t_1}^H, \dots, B_{t_\nu}^H)^\top] + R_{1,\nu} R_\nu^{-1} (B_{t_1}^H, \dots, B_{t_\nu}^H)^\top \\ &= R_{1,\nu} R_\nu^{-1} (B_{t_1}^H, \dots, B_{t_\nu}^H)^\top \\ &= (r_H(t_1, t), \dots, r_H(t_\nu, t)) R_\nu^{-1} (B_{t_1}^H, \dots, B_{t_\nu}^H)^\top \\ &= \frac{1}{2} (t^{2H} + t_1^{2H} - (t - t_1)^{2H}, \dots, t^{2H} + t_\nu^{2H} - (t - t_\nu)^{2H}) R_\nu^{-1} \\ &\quad \cdot (B_{t_1}^H, \dots, B_{t_\nu}^H)^\top. \end{aligned}$$

This function is differentiable in t and we get

$$f(s, \tau(t), \tilde{B}^{H, \leq \tau(t)}) = H(s^{2H-1} - (s-t_1)^{2H-1}, \dots, s^{2H-1} - (s-t_\nu)^{2H-1}) R_\nu^{-1} (B_{t_1}^H, \dots, B_{t_\nu}^H)^\top,$$

where $\tau(t) = t_\nu$ under the assumptions above.

The following result, which is a consequence of the upper bounds on Pickands constant (Shao, 1996; Debicki & Kisowski, 2008), shows that the running maximum process of fractional Brownian motion is L^p -integrable for all $1 \leq p < \infty$.

Proposition 6.12. *Let $H \in (0, 1]$ and B^H a fractional Brownian motion with Hurst parameter H . Let $X_T^* := (B_T^H)^* = \sup_{0 \leq t \leq T} |B_t^H|$ and $1 \leq p < \infty$. Then $\mathbb{E}[(X_T^*)^p] < \infty$.*

Proof. Pickands constant is defined as

$$\mathcal{H}_H := \lim_{t \rightarrow \infty} \frac{1}{t} \mathcal{H}_H(t), \quad \text{where} \quad \mathcal{H}_H(t) := \mathbb{E} \left[\exp \left(\sup_{0 \leq s \leq t} \left(\sqrt{2} B_s^H - s^{2H} \right) \right) \right].$$

According to (Debicki & Kisowski, 2008), \mathcal{H}_H is finitely bounded from above for every $H \in (0, 1]$, therefore, there exists some T_0 such that for all $t \geq T_0$, $\mathcal{H}_H(t)$ is finite and bounded from above by some constant. If $T < T_0$, we can use that $\mathbb{E}[(X_T^*)^p] \leq \mathbb{E}[(X_{T_0}^*)^p]$, hence we can assume without loss of generality that $T \geq T_0$. We have

$$\mathcal{H}_H(T) \geq \mathbb{E} \left[\exp \left(\sup_{0 \leq t \leq T} \left(\sqrt{2} B_t^H - T^{2H} \right) \right) \right] = \mathbb{E} \left[\exp \left(\sqrt{2} \sup_{0 \leq t \leq T} B_t^H \right) \right] \exp(-t^{2H})$$

and since B^H is symmetric around 0, implying that $-B^H \stackrel{d}{=} B^H$,

$$\mathbb{E} \left[\exp \left(\sqrt{2} X_T^* \right) \right] = \mathbb{E} \left[\exp \left(\sqrt{2} \sup_{0 \leq t \leq T} |B_t^H| \right) \right] \leq 2 \mathbb{E} \left[\exp \left(\sqrt{2} \sup_{0 \leq t \leq T} B_t^H \right) \right] + 2.$$

Together, this implies that $\mathbb{E} \left[\exp \left(\sqrt{2} X_T^* \right) \right] < \infty$, which means that the moment generating function of X^* is finite. A well known property of the moment generating function implies that

$$\mathbb{E}[(X_T^*)^p] \leq \left(\frac{p}{\sqrt{2}e} \right)^p \mathbb{E} \left[\exp \left(\sqrt{2} X_T^* \right) \right] < \infty,$$

since X_T^* is non-negative. □

6.6 MULTIVARIATE PROCESS WITH INCOMPLETE OBSERVATIONS: CORRELATED BROWNIAN MOTIONS

Let A, B, C be three i.i.d. 1-dimensional Brownian motions and let $\alpha, \beta > 0$ with $\alpha^2 + \beta^2 = 1$. Then we define the process $X := (U, V)^\top := (\alpha A + \beta B, \alpha A + \beta C)^\top$. U, V are again Brownian motions, but they are correlated. First we remark, that $\mathbb{E}[(X_T^*)^p] < \infty$ for every $1 \leq p < \infty$ (cf. (Cohen & Elliott, 2015, Lemma 16.1.4)).

In this example we assume to have incomplete observations. In particular, we allow for observation times at which only U or only V is observed. Therefore, let us define the (ordered) observations of U as r_i for $1 \leq i \leq n_U$ and those of V as s_i for $1 \leq i \leq n_V$, where n_U, n_V are random variables similar to n , representing the total number of observations of U and V respectively. As before, t_i for $1 \leq i \leq n$ are the times at which observations are made, i.e., the times at which at least one of U, V is observed. Due to the correlation of the coordinates, observing (only) one coordinate, generally also impacts the conditional expectation of the other one. To compute the true conditional expectations given the discrete (possibly incomplete) previous observations, we use the fact, that the increments of A, B, C are independent Gaussian random variables. Remember that $t_0 = 0$ and let $\tilde{A}_i := A_{t_i} - A_{t_{i-1}}$ for all $1 \leq i \leq n$ and similar for B, C . Then we define

$$v := (\tilde{A}_1, \dots, \tilde{A}_n, \tilde{B}_1, \dots, \tilde{B}_n, \tilde{C}_1, \dots, \tilde{C}_n)^\top,$$

which is multivariate normally distributed with $v \sim N(0, \Sigma)$, where

$$\Sigma := \text{diag}(t_1 - t_0, \dots, t_n - t_{n-1}, t_1 - t_0, \dots, t_n - t_{n-1}, t_1 - t_0, \dots, t_n - t_{n-1}).$$

Let $I_l \in \mathbb{R}^{n \times n}$ be the lower triangular matrix with all ones and define the matrix

$$\tilde{\Gamma} := \begin{pmatrix} \alpha I_l & \beta I_l & 0 \\ \alpha I_l & 0 & \beta I_l \end{pmatrix} \in \mathbb{R}^{2n \times 3n}.$$

Then $(U_{t_1}, \dots, U_{t_n}, V_{t_1}, \dots, V_{t_n})^\top = \tilde{\Gamma}v$. Let $t > 0$ be the current time and let $k \in \mathbb{N}$ be such that $t_k \leq t < t_{k+1}$, where $t_{n+1} := \infty$. Moreover, let $k_U, k_V \in \mathbb{N}$ be such that $r_{k_U} \leq t_k < r_{k_U+1}$ and $s_{k_V} \leq t_k < s_{k_V+1}$. In the following we compute conditional expectations of V . Those of U follow equivalently. First we notice, that the independent increments of Brownian motion imply

$$\mathbb{E}[V_t | \mathcal{A}_t] = \mathbb{E}[V_t - V_{t_k} | \mathcal{A}_{t_k}] + \mathbb{E}[V_{t_k} | \mathcal{A}_{t_k}] = \mathbb{E}[V_{t_k} | \mathcal{A}_{t_k}] = \mathbb{E}[V_{t_k} | U_{r_1}, \dots, U_{r_{k_U}}, V_{s_1}, \dots, V_{s_{k_V}}]$$

and therefore, $f(s, \tau(t), \tilde{X}^{\leq \tau(t)}) = 0$. If $s_{k_V} = t_k$, i.e., if V_{t_k} was observed, then $\mathbb{E}[V_{t_k} | \mathcal{A}_{t_k}] = V_{t_k}$. Otherwise, $s_{k_V} < t_k$ and we define

$$\Upsilon := \text{diag}(\mathbf{1}_{\{t_1 \in \mathcal{R}\}}, \dots, \mathbf{1}_{\{t_n \in \mathcal{R}\}}, \mathbf{1}_{\{t_1 \in \mathcal{S}\}}, \dots, \mathbf{1}_{\{t_n \in \mathcal{S}\}}),$$

where $\mathcal{R} := \{r_1, \dots, r_{k_U}\}$ and $\mathcal{S} := \{s_1, \dots, s_{k_V}\} \cup \{t_k\}$, as well as $\tilde{\Upsilon}$ as the submatrix of Υ with all rows with only 0-entries removed. For $\Gamma := \tilde{\Upsilon}\Upsilon$ we therefore have

$$(U_{r_1}, \dots, U_{r_{k_U}}, V_{s_1}, \dots, V_{s_{k_V}}, V_{t_k})^\top = \Gamma v \sim N(0, \Gamma \Sigma \Gamma^\top),$$

where we used a well known fact about affine transformations of multivariate normal distributions (see e.g. (Eaton, 2007, Chapter 3.1)). Let

$$\tilde{\Sigma} := \Gamma \Sigma \Gamma^\top =: \begin{pmatrix} \tilde{\Sigma}_{11} & \tilde{\Sigma}_{12} \\ \tilde{\Sigma}_{21} & \tilde{\Sigma}_{22} \end{pmatrix},$$

where $\tilde{\Sigma}_{11} \in R^{k_U+k_V, k_U+k_V}$, $\tilde{\Sigma}_{12} = \tilde{\Sigma}_{21}^\top \in R^{k_U+k_V, 1}$ and $\tilde{\Sigma}_{22} = \text{Var}(V_{t_k}) \in R$. Then, the conditional distribution of $(V_{t_k} | U_{r_1}, \dots, U_{r_{k_U}}, V_{s_1}, \dots, V_{s_{k_V}})$ is again normal with mean $\hat{\mu} := \tilde{\Sigma}_{21} \tilde{\Sigma}_{11}^{-1} (U_{r_1}, \dots, U_{r_{k_U}}, V_{s_1}, \dots, V_{s_{k_V}})^\top$ and variance $\hat{\Sigma} := \tilde{\Sigma}_{22} - \tilde{\Sigma}_{21} \tilde{\Sigma}_{11}^{-1} \tilde{\Sigma}_{12}$ (Eaton, 2007, Proposition 3.13)). In particular, we have $\mathbb{E}[V_{t_k} | \mathcal{A}_{t_k}] = \hat{\mu}$.

7 EXPERIMENTS

The code with all new experiments and those from (Herrera et al., 2021) is available at <https://github.com/FlorianKrach/PD-NJODE>. Further details about the experiments can be found in Appendix A.

First we use synthetic datasets to confirm our theoretical results for all generalizations of the problem settings over those in (Herrera et al., 2021). In particular, we show that the path-dependent NJ-ODE can be applied successfully when the underlying process has jumps (Section 7.1) or is path dependent (Section 7.4), when observations are incomplete (Section 7.5) or observation times depend on the value of the process (Section 7.3). Moreover, we verify that the (path-dependent) NJ-ODE can be used for uncertainty estimation as was suggested in Section 5. The model performance is measured by the *evaluation metric* that was introduced in (Herrera et al., 2021, Sec. 6.1). This metric computes the MSE on a discretization time grid between the optimal prediction (given by the conditional expectation) and the predictions of the model on the samples of the test set. It is given by

$$\text{eval}(\hat{X}, Y^\theta) := \frac{1}{N_2} \sum_{j=1}^{N_2} \frac{1}{\kappa + 1} \sum_{i=0}^{\kappa} \left(\hat{X}_{\frac{iT}{\kappa}}^{(j)} - Y_{\frac{iT}{\kappa}}^{\theta, j} \right)^2,$$

where the outer sum runs over the test set of size N_2 and the inner sum runs over the equidistant grid points on the time interval $[0, T]$.

In Section 7.1 and 7.2 we show results using the standard NJ-ODE model, since the respective datasets do not exhibit any of the complications that would require (numerically) the PD-NJ-ODE. However, we remark that PD-NJ-ODE leads (at least) to the same quality of results.

Our empirical results on more complicated datasets suggest, that using the equivalent objective function as described in Remark 4.6 is preferable, since the training is more stable. Our explanation for this is, that with the original loss function, the training more easily ends up in local optima which are not global optima. However, these local optima do not exist for the equivalent loss function due to its slightly different structure, hence the training does not end up there. For more details see Appendix A.1.4.

Finally, in Section 7.6 and Section 7.7 we apply the PD-NJ-ODE model to real world datasets. First, to the PhysioNet dataset of patient health parameters, where the results of PD-NJ-ODE are compared to those of NJ-ODE. And then to 3 datasets of limit order book (LOB) data, where the architecture of the PD-NJ-ODE is adapted to additionally address a classification task.

7.1 PROCESS WITH JUMPS – POISSON POINT PROCESS

In this experiment we use a Poisson point process, that was described in Section 6.4, to show that NJ-ODE can successfully be applied to processes with jumps. Already the standard NJ-ODE model without extensions leads to an evaluation metric smaller than $2 \cdot 10^{-5}$ after only 30 epochs of training (Figure 1). Hence, we conclude that this is another problem setting, where no extension of NJ-ODE model is needed although the setting is not covered by the theoretical framework in (Herrera et al., 2021) (as is the case for Black–Scholes, Ornstein-Uhlenbeck and Heston processes as well).

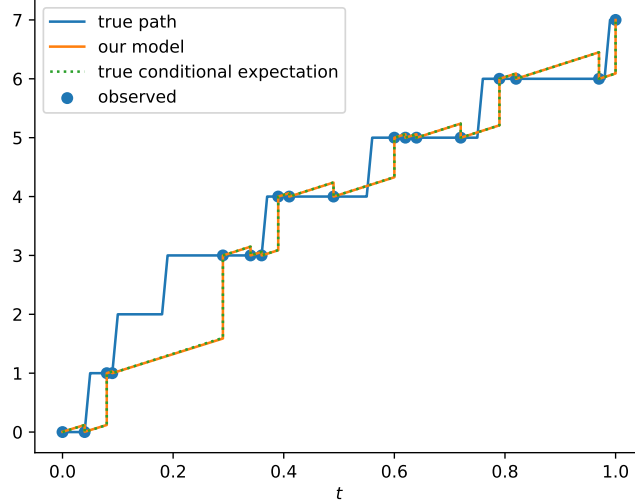


Figure 1: Predicted and true conditional expectation on a test sample of the Poisson point process. All upward movements of the true path are jumps, the slope is only due to the discretization time grid.

7.2 UNCERTAINTY ESTIMATION – BROWNIAN MOTION AND ITS SQUARE

We apply NJ-ODE to a Brownian motion X and its square X^2 , as described in Example 5.1, to show that our model can be used to compute the conditional variance, which gives rise to an uncertainty estimate of the prediction. In Figure 2, we show the predictions of the 2-dim process (X, X^2) as well as the prediction of X together with a confidence region defined as $\hat{\mu}_t \pm \hat{\sigma}_t$, where $\hat{\mu}_t$ is NJ-ODE's predicted conditional expectation and $\hat{\sigma}_t^2$ is its predicted conditional variance at time t . The evaluation metric on the 2-dimensional dataset becomes smaller than $5 \cdot 10^{-5}$.

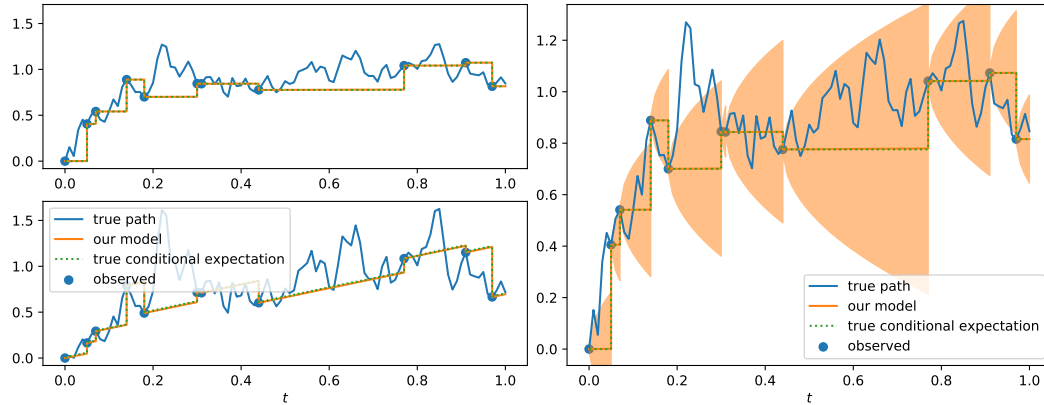


Figure 2: Left: a test sample of a Brownian motion X (top) and its square X^2 (bottom) together with the predicted and true conditional expectation. Right: the same test sample of the Brownian motion X with a confidence interval given as $\hat{\mu}_t \pm \hat{\sigma}_t$.

Table 1: Minimal evaluation metrics on the test set of FBM (with $H = 0.05$) within the 200 epochs of training for different NJ-ODE models.

	NJ-ODE	NJ-ODE (with sig.)	NJ-ODE (with RNN)	PD-NJ-ODE
min. evaluation metric	$8.1 \cdot 10^{-2}$	$1.0 \cdot 10^{-2}$	$1.1 \cdot 10^{-2}$	$0.5 \cdot 10^{-2}$

7.3 OBSERVATION INTENSITY DEPENDING ON THE UNDERLYING PROCESS

For a Black–Scholes model X , we use the following method to randomly sample observation times. As usual, the process is sampled on a grid with step size 0.01 and for each of the grid points an independent Bernoulli random variable is drawn to determine whether it is used as observation time or not (cf. Appendix A.1.2). The only difference is, that the success probability of the Bernoulli random variable is $p = 0.05 + 0.4 \tanh(|X_t|/10)$, where X_t is the value of the process at the given grid point. The PD-NJ-ODE model applied to this dataset, learns to correctly predict the process (Figure 3) achieving a minimal evaluation metric of $6.2 \cdot 10^{-4}$.

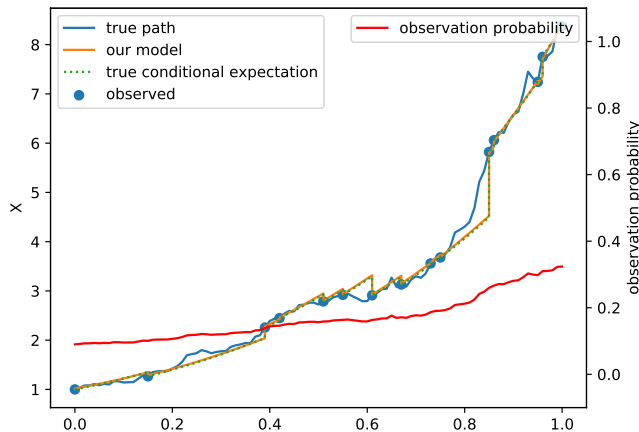


Figure 3: Predicted and true conditional expectation on a test sample of the Black–Scholes dataset, where the observation intensity depends on the values of the process.

7.4 PATH DEPENDENT PROCESS – FRACTIONAL BROWNIAN MOTION

Path dependent processes are one of the main application areas for the extension of NJ-ODE. Here we use a fractional Brownian motion (FBM) with Hurst parameter $H = 0.05$, which yields a rough process with high negative auto-correlation (cf. Section 6.5). To show that PD-NJ-ODE performs better than the standard NJ-ODE, we compare them as well as 2 intermediate versions, where once the signature is added as input to NJ-ODE and once a recurrent jump network is used in NJ-ODE. For all 4 models the same architecture is used. The optimal evaluation metric for each of the models is given in Table 1. PD-NJ-ODE achieves the best evaluation metric, for the two intermediate models it is approximately doubled and for NJ-ODE it is about 16 times larger.

Although our theoretical results imply, that the NJ-ODE with signature should be enough, the performance can depend on the truncation level used for the signature input. All truncation levels between $m \in \{1, \dots, 10\}$ were tested. For $m = 1$ and $m = 2$ the minimal evaluation metric was $1.1 \cdot 10^{-2}$ and $0.6 \cdot 10^{-2}$. For all $m \geq 3$, it was $0.5 \cdot 10^{-2}$. The computation time grows with increasing truncation level m , since it depends on the input dimension of the neural networks which increases according to (4) for growing m . Therefore, we choose to use a truncation level of 2 or 3 for all of our experiments, since this seems to be a good trade-off between model performance and computation time. Here we report results with $m = 3$.

Since truncation levels up to $m = 10$ are still rather small, it is not surprising that using the recurrent structure can carry on additional path information that is not covered by the truncated signature and

therefore leads to improved quality.

On the other hand these results also show, that the recurrent structure alone does not carry all necessary path information. These differences in the quality of the predictions can also be seen in Figure 4.

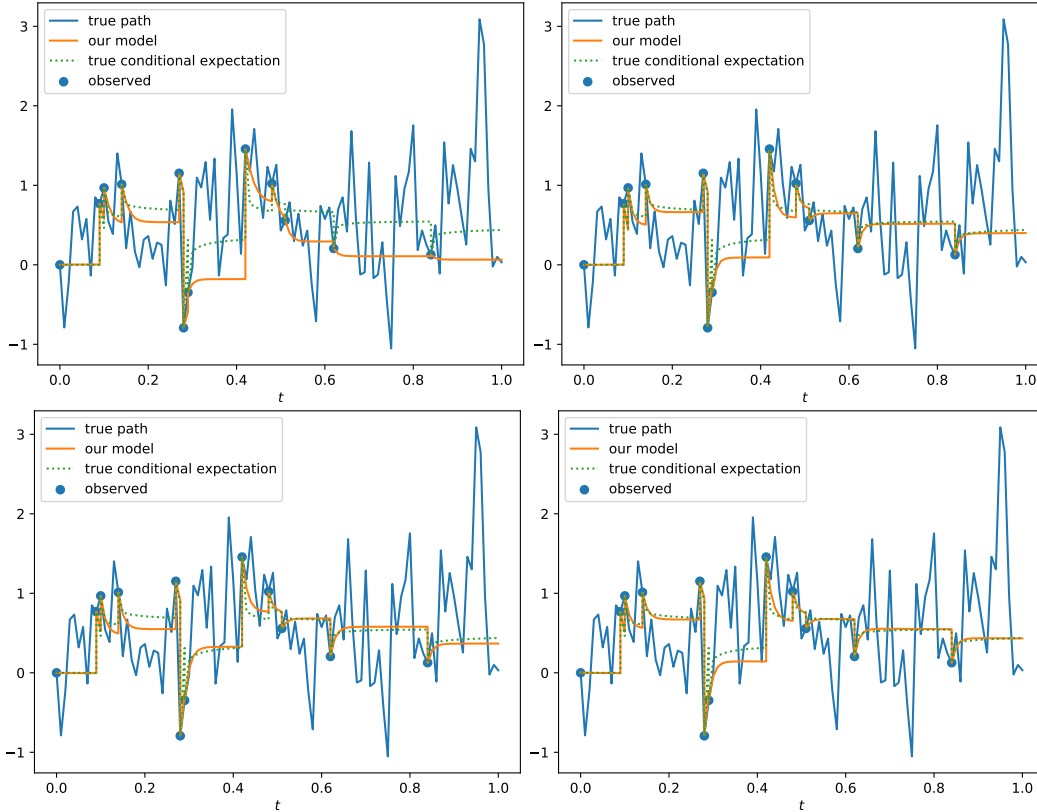


Figure 4: NJ-ODE (top-left), NJ-ODE with signature input (top-right), NJ-ODE with recurrent jump network (bottom-left) and PD-NJ-ODE (bottom-right) on a test sample of a fractional Brownian motion with Hurst parameter $H = 0.05$.

7.5 INCOMPLETE OBSERVATIONS – CORRELATED 2-DIMENSION BROWNIAN MOTION

To test the model on a synthetic dataset with incomplete observations, we consider the example of a 2-dimensional correlated Brownian motion, as described in Section 6.6, with $\alpha^2 = 0.9$. From the discretization grid, we first sample observation times as usual and for each observation time one of the two coordinates is picked at random to be observed (cf. Appendix A.1.2, where $\lambda = \infty$ is used). The derivations in Section 6.6 show, that the incomplete observations also introduce some path dependence. The path-dependent NJ-ODE model achieves a minimal evaluation metric of $5.2 \cdot 10^{-3}$ and we see that it reacts well with its prediction of the one coordinate when the other coordinate is observed, even for multiple consecutive observations of the same coordinate (Figure 5).

7.6 PHYSIONET

We test the PD-NJ-ODE model on the extrapolation task of Rubanova et al. (2019) on the PhysioNet Challenge 2012 dataset (Goldberger et al., 2000) and compare it to the results of NJ-ODE. In Table 2 we see, that the PD-NJ-ODE outperforms the NJ-ODE. While the results for the PD-NJ-ODE are computed with 1-hidden layer neural networks with 50 hidden nodes, compared to 2-hidden layer networks with 50 hidden nodes for NJ-ODE, the amount of parameters is much larger, since the signature truncated at level 2 is used as additional input (for the 41-dimensional underlying process, this amounts to 1'723 additional inputs). These results suggest that there is some (small) path-dependence in the PhysioNet dataset, which could be dealt with by the PD-NJ-ODE model.

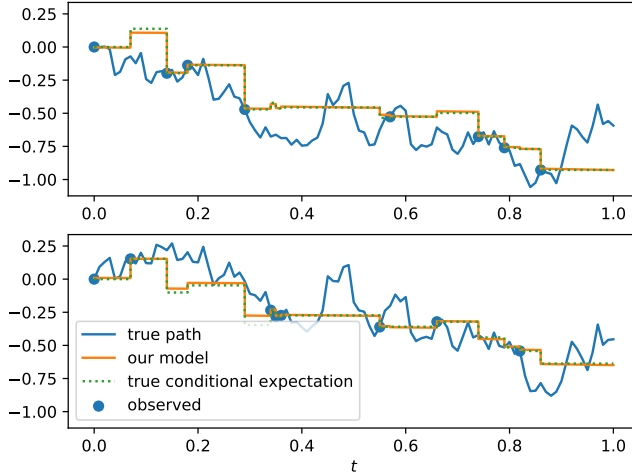


Figure 5: Predicted and true conditional expectation on a test sample of the 2-dimensional correlated Brownian motion (first coordinate plotted on top, second on bottom). The PD-NJ-ODE adjusts its prediction well for both coordinates when observing only one of them.

Table 2: Mean and standard deviation of MSE on the test set of physionet. Results of baselines were reported by [Rubanova et al. \(2019\)](#) and [Herrera et al. \(2021\)](#). Where known, the number of trainable parameters is reported.

	Physionet – MSE ($\times 10^{-3}$)	# params
RNN-VAE	3.055 ± 0.145	-
Latent ODE (RNN enc.)	3.162 ± 0.052	-
Latent ODE (ODE enc)	2.231 ± 0.029	163'972
Latent ODE + Poisson	2.208 ± 0.050	181'723
NJ-ODE	1.945 ± 0.007	24'423
PD-NJ-ODE	1.930 ± 0.006	201'691

7.7 LIMIT ORDER BOOK DATASETS

Stock and crypto-currency exchanges use a limit order book (LOB) to track all limit orders⁶ of agents who want to buy or sell any of the assets that are traded at the exchange. For each asset, the LOB has a buy and a sell side and for each side lists all the price levels together with the respective order volumes at which the agents would like to buy or sell. The midprice is defined as the mean between the best bid (buy order) and ask (sell order) price. The LOB of level $n \in \mathbb{N}$ is a truncated version of the LOB which only includes the n best (highest) bid and the n best (lowest) ask prices. In the following we always work with LOBs of level $n = 10$. Whenever a new order is made or an order is cancelled, the LOB is updated. New limit orders are added to the book, while new market orders are directly executed against the best available limit orders. Hence, LOBs are updated irregularly in time, making them a natural example to apply the PD-NJ-ODE.

We test our model on crypto-currency LOB data. The first dataset (denoted “BTC”) is based on one day of data of the LOB of Bitcoin, which was gratefully provided to us by Covario. The other datasets (denoted “BTC1sec” and “ETH1sec”) are based on roughly 12 days of snapshots of the LOB of Bitcoin (BTC) and Ethereum (ETH) at a frequency of 1 second (i.e. once every second the state of the LOB is saved instead of saving it at every update of the book). Using snapshots of the LOB at a predefined frequency usually leads to a loss of information compared to the full LOB. However, these datasets are publicly available ([Nielsen](#)), which is the reason why we include them here. For all datasets, any data point at which the first 10 levels of the LOB did not change compared

⁶A limit order is the order to buy (sell) a certain amount of an asset for some maximum (minimum) price or below (above).

Table 3: Minimal MSEs (smaller is better) during the training of each model (if applicable) are reported for different LOB datasets.

	BTC	BTC1sec	ETH1sec
last observation	0.11808	1350.44	2.58909
best linear regression	0.12198	1355.04	2.58253
PD-NJ-ODE	0.11743	1343.91	2.56636

Table 4: The true mean value and PD-NJ-ODE’s mean predicted value of the midprices 10 steps ahead for the 3 different datasets and their subsets by labels.

	BTC		BTC1sec		ETH1sec	
	true	prediction	true	prediction	true	prediction
overall	0.01143	0.01123	-2.40790	-2.39125	-0.12932	-0.10787
decrease	-0.41470	-0.31175	-47.28358	-28.80446	-2.19563	-1.25667
stationary	0.08016	0.08585	-2.75307	-3.27602	-0.34508	-0.36719
increase	0.44849	0.31417	40.63428	23.33839	2.24031	1.30459

to the previous one is deleted. The datasets are split into non-overlapping samples, which have 100 consecutive data points as input and the data point 10 steps ahead as label to be predicted.

The common task in the literature is to predict price movements, i.e., whether the midprice increases, decreases or stays roughly constant (Tran et al., 2017; Tsantekidis et al., 2017; Dixon et al., 2017; Ntakaris et al., 2018; Passalis et al., 2018; Tsantekidis et al., 2020; Zhang et al., 2019). As a baseline, we use the state-of-the-art DeepLOB model (Zhang et al., 2019), which was shown to outperform a large amount of other models (i.e. Ridge Regression, Single-Layer Feedforward Networks, Linear Discriminant Analysis, Multilinear Discriminant Analysis, Multilinear Time-series Regression, Multilinear Class-specific Discriminant Analysis, Bag-of-Features, Neural Bag-of-Features and Attention-augmented-Bilinear-Networks with one and two hidden layers).

To compare to these results, we extend the PD-NJ-ODE model by a classifier network, which maps the latent variable H_{t_n} after the last data point was processed to the probabilities that the 10-steps ahead label belongs to one of the classes (increase, decrease, stationary). This classifier network is trained using a cross-entropy loss, first together with the remaining PD-NJ-ODE architecture and afterwards again on its own. The reason why the classifier is retrained is, that the training of the PD-NJ-ODE model is relatively time-consuming, while training the classifier alone is very fast. Since the 50 epochs for which the PD-NJ-ODE is trained are not sufficient for the classifier to reach its best performance, we retrain it for another 1000 epochs on its own.

The natural task for our model is the regression problem to forecast the value of the midprice 10-steps ahead. Due to a lack of baseline models in the literature for this task, we compare the midprice prediction of PD-NJ-ODE to 2 simple baselines. First, we use the midprice of the last observation as prediction for the midprice 10 steps ahead, i.e. the stationary prediction. And secondly, we fit linear regression models on the entire training data or subsets of it (only midprices and bid/ask prices but no volumes, only midprices, only midprices of last 10 observation dates, only midprice of last observation date). For all datasets, the best linear regression model is the one using only the midprice of the last observation, therefore only results of this model are reported.

In Table 3 we see, that in the regression task the PD-NJ-ODE model outperforms the best baseline method by about 0.5% in each of the three datasets. Although this outperformance is relatively small, it is important to note that in both Bitcoin datasets all linear regression models do worse than the stationary prediction and in the Ethereum dataset only the easiest linear model, using only the midprice of the last observation time as predictor, is slightly better than the stationary prediction. In particular this implies, that even very easy linear models overfit to the noise in the LOB data. On the contrary, the PD-NJ-ODE model manages to extract at least a little more information from the LOB paths without wrongly adapting to their noise. In Table 4 we show our model’s mean predicted value and the true mean value of the midprice 10 steps ahead for the entire datasets and for the subset

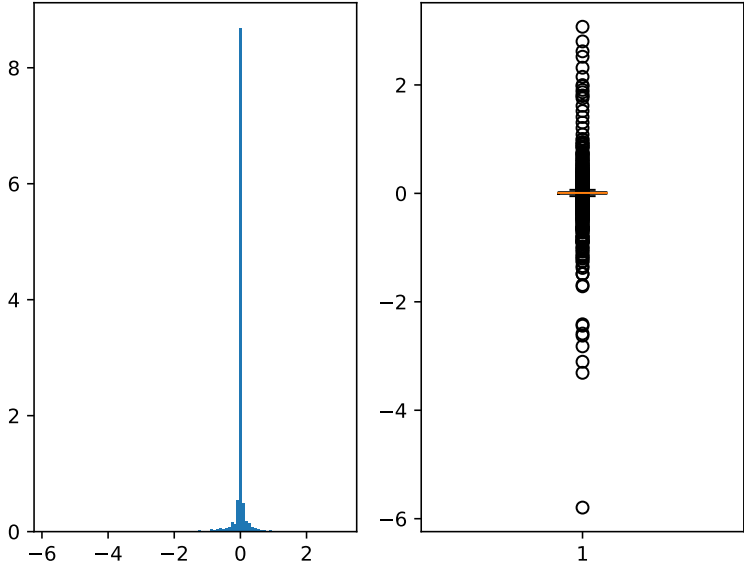


Figure 6: Distribution of the prediction errors of the PD-NJ-ODE model as (density) histogram and boxplot on the BTC dataset.

Table 5: Maximal F1-scores (in %, larger is better) during the training of each model are reported for different LOB datasets.

	BTC	BTC1sec	ETH1sec
DeepLOB	61.59	52.24	44.97
PD-NJ-ODE (no retraining)	52.34	52.02	52.48
PD-NJ-ODE (classifier retrained)	62.06	no improvement	54.08

of the three different labels. Taking the means is a good way to average out the random noise of the samples. But, at the same time, also some true information is averaged out (see for example the difference between overall mean and the means of the three labels). For all three datasets we see that the overall mean prediction is relatively close to the true mean, while the absolute values of the mean predictions for decrease and increase labels are significantly smaller than the true ones. This can be explained with the boxplot of the prediction errors (i.e. the differences between predicted values and the respective true values) shown in Figure 6 for the BTC dataset and in Figure 8 in the Appendix for the other two datasets. Although the distributions are concentrated closely around 0, there are many large outliers on both sides, which increase the true absolute means for decrease and increase labels. On the other hand, the PD-NJ-ODE model seems to learn the main behaviour without overfitting to these large valued outliers, which keeps the predicted absolute means smaller in those two groups. In particular, this suggests that the PD-NJ-ODE is a robust and flexible model at the same time.

The results of the classification task for the three datasets are shown in Table 5, where we compare the weighted F1-scores of the models, as it was done by Zhang et al. (2019). For the two Bitcoin datasets, the PD-NJ-ODE (with retrained classifier) and DeepLOB yield very similar results. On the Ethereum dataset, our model achieves slightly better results than on “BTC1sec”, while the DeepLOB model performs significantly worse, for which we do not have an explanation⁷. Overall we conclude, that even though classification is not the core task of our model, the results are very promising already with a simple classifier network that is added on top of the PD-NJ-ODE model.

⁷The DeepLOB model was trained several times to exclude the possibility that this was due to an unfortunate initialization or something similar.

8 CONCLUSION

We extended the NJ-ODE model to work for much more general datasets and settings. In (Herrera et al., 2021) there were examples for which NJ-ODE worked well empirically, although they were not covered by the theoretical settings. Here, we brought the theoretical and empirical results to the same level, by giving the weakest possible constraints on the data process such that PD-NJ-ODE can be applied successfully. Indeed, if the continuous differentiability of the conditional expectation is not satisfied, it is clear that the proposed framework cannot approximate it arbitrarily well, since neural networks cannot approximate the corresponding functions arbitrarily well. On the other hand, if the integrability assumption is not satisfied, the loss function is not well defined. Moreover, we showed empirically, using multiple synthetic datasets, that the PD-NJ-ODE truly works in all of these more complicated settings, that the theoretical results permit now. Finally, the application of PD-NJ-ODE to limit order book data yielded very promising results, which will be elaborated further in future work.

ACKNOWLEDGEMENT

The authors thank Andrew Allan, Robert A. Crowell and Calypso Herrera for helpful discussions and feedback. Moreover, they thank William Andersson for his very careful proofreading. The authors also want to thank Covario for providing the LOB BTC dataset.

REFERENCES

- Leif BG Andersen and Vladimir V Piterbarg. Moment explosions in stochastic volatility models. *Finance and Stochastics*, 11(1):29–50, 2007.
- Jürgen Appell, Józef Banas, and Nelson José Merentes Díaz. Bounded variation and around. In *Bounded Variation and Around*. de Gruyter, 2013.
- Patrick Billingsley. *Probability and Measure*. J. Wiley, third ed. edition, 1995.
- Patric Bonnier, Patrick Kidger, Imanol Perez Arribas, Cristopher Salvi, and Terry Lyons. Deep signature transforms. *arXiv*, 2019.
- Edward De Brouwer, Jaak Simm, Adam Arany, and Yves Moreau. GRU-ODE-Bayes: Continuous modeling of sporadically-observed time series. *NeurIPS*, 2019.
- Dariusz Bugajewski and Jacek Gulowski. On the characterization of compactness in the space of functions of bounded variation in the sense of jordan. *Journal of Mathematical Analysis and Applications*, 484(2), 2020.
- Wei Cao, Dong Wang, Jian Li, Hao Zhou, Lei Li, and Yitan Li. Brits: Bidirectional recurrent imputation for time series. *Advances in Neural Information Processing Systems*, 31, 2018.
- Zhengping Che, Sanjay Purushotham, Kyunghyun Cho, David Sontag, and Yan Liu. Recurrent neural networks for multivariate time series with missing values. *Scientific Reports*, 8, 2018.
- Ricky T. Q. Chen, Yulia Rubanova, Jesse Bettencourt, and David Duvenaud. Neural ordinary differential equations. *NeurIPS*, 2018.
- Ilya Chevyrev and Andrey Kormilitzin. A primer on the signature method in machine learning. *ArXiv*, abs/1603.03788, 2016.
- Samuel N Cohen and Robert James Elliott. *Stochastic calculus and applications*. Springer, 2015.
- Krzysztof Debicki and Pawel Kisowski. A note on upper estimates for pickands constants. *Statistics & Probability Letters*, 78(14):2046–2051, 2008.
- Matthew Dixon, Diego Klabjan, and Jin Hoon Bang. Classification-based financial markets prediction using deep neural networks. *Algorithmic Finance*, 6(3-4):67–77, 2017.
- Rick Durrett. *Probability: Theory and Examples*. Cambridge University Press, 2010.

- Morris L Eaton. *Multivariate Statistics: A Vector Space Approach*. Institute of Mathematical Statistics, 2007.
- Adeline Fermanian. Embedding and learning with signatures, 2020.
- Ary L. Goldberger, Luis A. N. Amaral, Leon Glass, Jeffrey M. Hausdorff, Plamen Ch. Ivanov, Roger G. Mark, Joseph E. Mietus, George B. Moody, Chung-Kang Peng, and H. Eugene Stanley. Physiobank, physiotookit, and physionet. *Circulation*, 2000.
- Massimiliano Gubinelli. Stochastic analysis - course note 4. *Lecture Notes* https://www.iam.uni-bonn.de/fileadmin/user_upload/gubinelli/stochastic-analysis-ss16/sa-note-4.pdf, 2016.
- Calypso Herrera, Florian Krach, and Josef Teichmann. Neural jump ordinary differential equations: Consistent continuous-time prediction and filtering. In *International Conference on Learning Representations*, 2021.
- Kurt Hornik, Maxwell Stinchcombe, and Halbert White. Multilayer feedforward networks are universal approximators. *Neural Networks*, 2, 1989.
- Michael I Jordan. Serial order: A parallel distributed processing approach. In *Advances in Psychology*, volume 121. Elsevier, 1997.
- Martin Keller-Ressel. Moment explosions and long-term behavior of affine stochastic volatility models. *Mathematical Finance: An International Journal of Mathematics, Statistics and Financial Economics*, 21(1):73–98, 2011.
- Patrick Kidger, James Morrill, James Foster, and Terry Lyons. Neural controlled differential equations for irregular time series. *Advances in Neural Information Processing Systems*, 33, 2020.
- Franz J. Kiraly and Harald Oberhauser. Kernels for sequentially ordered data. *Journal of Machine Learning Research*, 20(31):1–45, 2019.
- Bernard Lapeyre and Jérôme Lelong. Neural network regression for bermudan option pricing. *Monte Carlo Methods and Applications*, 27(3):227–247, 2021.
- Martin Sogaard Nielsen. High frequency crypto limit order book data. URL <https://www.kaggle.com/datasets/martinsn/high-frequency-crypto-limit-order-book-data>.
- Ilkka Norros, Esko Valkeila, and Jorma Virtamo. An elementary approach to a Girsanov formula and other analytical results on fractional Brownian motions. *Bernoulli*, 5(4):571 – 587, 1999.
- Adamantios Ntakaris, Martin Magris, Juho Kannianen, Moncef Gabbouj, and Alexandros Iosifidis. Benchmark dataset for mid-price forecasting of limit order book data with machine learning methods. *Journal of Forecasting*, 37(8):852–866, 2018.
- Nikolaos Passalis, Anastasios Tefas, Juho Kannianen, Moncef Gabbouj, and Alexandros Iosifidis. Temporal bag-of-features learning for predicting mid price movements using high frequency limit order book data. *IEEE Transactions on Emerging Topics in Computational Intelligence*, 4(6): 774–785, 2018.
- Philip Protter. Stochastic integration and differential equations. *Springer-Verlag*, 2005.
- Jeremy Reizenstein and Benjamin Graham. The iisignature library: efficient calculation of iterated-integral signatures and log signatures. *arXiv*, 2018.
- Yulia Rubanova, Ricky T. Q. Chen, and David K Duvenaud. Latent ordinary differential equations for irregularly-sampled time series. *NeurIPS*, 2019.
- David E Rumelhart, Geoffrey E Hinton, and Ronald J Williams. Learning internal representations by error propagation. Technical report, California Univ San Diego La Jolla Inst for Cognitive Science, 1985.

- Qi-Man Shao. Bounds and estimators of a basic constant in extreme value theory of gaussian processes. *Statistica Sinica*, 6(1):245–257, 1996.
- Tommi Sottinen and Lauri Viitasaari. Prediction law of fractional brownian motion. *arXiv*, 2017.
- Gunnar Taraldsen. Optimal learning from the doob-dynkin lemma. *arXiv*, 2018.
- Dat Thanh Tran, Martin Magris, Juho Kanninen, Moncef Gabbouj, and Alexandros Iosifidis. Tensor representation in high-frequency financial data for price change prediction. In *2017 IEEE Symposium Series on Computational Intelligence (SSCI)*, pp. 1–7. IEEE, 2017.
- Avraam Tsantekidis, Nikolaos Passalis, Anastasios Tefas, Juho Kanninen, Moncef Gabbouj, and Alexandros Iosifidis. Forecasting stock prices from the limit order book using convolutional neural networks. In *2017 IEEE 19th conference on business informatics (CBI)*, volume 1, pp. 7–12. IEEE, 2017.
- Avraam Tsantekidis, Nikolaos Passalis, Anastasios Tefas, Juho Kanninen, Moncef Gabbouj, and Alexandros Iosifidis. Using deep learning for price prediction by exploiting stationary limit order book features. *Applied Soft Computing*, 93:106401, 2020.
- Zihao Zhang, Stefan Zohren, and Stephen Roberts. Deeplob: Deep convolutional neural networks for limit order books. *IEEE Transactions on Signal Processing*, 67(11):3001–3012, 2019.

A EXPERIMENTAL DETAILS

A.1 IMPLEMENTATION DETAILS

A.1.1 REMARKS ON THE SIGNATURE

First we note that the “not-tree-like” condition is easily fulfilled in practice by having a monotonously increasing coordinate in the data. To this end, we concatenate the current time as additional dimension to the data, which is standard procedure when working with signatures (see for example (Fermanian, 2020)). If the function to be learnt in Theorem 3.7 depends significantly on higher degree terms, and the truncation level is chosen too low, some information will inevitably be lost. For a more elaborate setup, Bonnier et al. (2019) discuss methods to reduce this issue by applying an augmentation to the original data stream before computing the signature. In our applications, we deal with this issue in another way. We use a recurrent structure, which can learn to extract and store certain path-dependent feature of the data. In particular, this could learn to approximate some higher degree term of the signature, which carries significant information

To actually compute the signature (of the interpolated paths we consider), multiple python packages are available, as for example *ESig*, *iisignature* and *signatory*. For our implementation, we use the great *iisignature* package implemented by Reizenstein & Graham (2018).

A.1.2 SYNTHETIC DATASETS

We use the same method to generate datasets as in (Herrera et al., 2021). In particular, if not mentioned otherwise, we consider the time interval $[0, 1]$, i.e., $T = 1$, and a discretization time grid with step size 0.01 which leads to 101 time points on this interval. For each path i and each of these time points t , an independent Bernoulli random variable $O_{i,t} \sim \text{Bernoulli}(p)$ is drawn and the time point is used as observation time if $O_{i,t} = 1$. Our standard choice for the success probability is $p = 0.1$. The paths themselves are sampled by either using a closed form method if available or the euler scheme adapted to the discretization time grid. The standard choice is to sample a set of 20'000 paths which is split into 80% training set and 20% test set.

For synthetic datasets with incomplete observations (i.e. masked data) for each of the observation times (i.e. where $O_{i,t} = 1$), first an independent random variable $N_{i,t} \sim 1 + \text{Poisson}(\lambda)$ is drawn which specifies the amount of coordinates observed at this time, and then $\min(d_X, N_{i,t})$ coordinates are drawn at random (without replacement) from the set of all coordinates, to be the observed ones. If $\lambda = \infty$, then exactly one (randomly chosen) coordinate is observed at each observation time.

A.1.3 TRAINING

We always use the Adam optimizer with the standard choices $\beta = (0.9, 0.999)$ and weight decay of 0.0005. If not mentioned otherwise, our standard choice for the learning rate is 0.001, a dropout rate of 0.1 is used for every layer and training is performed with a mini-batch size of 200 for 200 epochs.

A.1.4 OBJECTIVE FUNCTION

The (original) loss function (6),

$$\Psi : \mathbb{D} \rightarrow \mathbb{R}, Z \mapsto \Psi(Z) := \mathbb{E}_{\mathbb{P} \times \tilde{\mathbb{P}}} \left[\frac{1}{n} \sum_{i=1}^n (|M_t \odot (X_{t_i} - Z_{t_i})|_2 + |M_t \odot (Z_{t_i} - Z_{t_i-})|_2)^2 \right],$$

uses the distance between the prediction before and after the jump, to make the neural ODE learn the correct behaviour between the jumps. In contrast, the equivalent loss function (cf. Remark 4.6),

$$\tilde{\Psi} : \mathbb{D} \rightarrow \mathbb{R}, Z \mapsto \tilde{\Psi}(Z) := \mathbb{E}_{\mathbb{P} \times \tilde{\mathbb{P}}} \left[\frac{1}{n} \sum_{i=1}^n (|M_t \odot (X_{t_i} - Z_{t_i})|_2 + |M_t \odot (X_{t_i} - Z_{t_i-})|_2)^2 \right],$$

uses the distance between the observation and the prediction before the jump. As can be seen in the left plot of Figure 7, with the original loss function, there can be local minima, at which the model doesn't jump to X_{t_i} at a new observation, but to a point between X_{t_i} and Z_{t_i-} , at which the term $(Z_{t_i} - Z_{t_i-})$ is smaller than it would be for $Z_{t_i} = X_{t_i}$. The model achieves a minimal evaluation

metric of $1.8 \cdot 10^{-2}$ for the weights being stuck at this local minimum. For the equivalent loss function, the value Z_{t_i-} before the jump is directly compared to X_{t_i} , such that jumping to a point $Z_{t_i} \neq X_{t_i}$ does not lead to any advantage locally (Figure 7 right). The model achieves a minimal evaluation metric of $1.0 \cdot 10^{-2}$, which is nearly an improvement by a factor of 2. The used models here are NJ-ODEs with the signature as additional input, both with the same architecture for each neural network with latent dimension $d_H = 50$ and 2 hidden layers with tanh activations and 200 nodes.

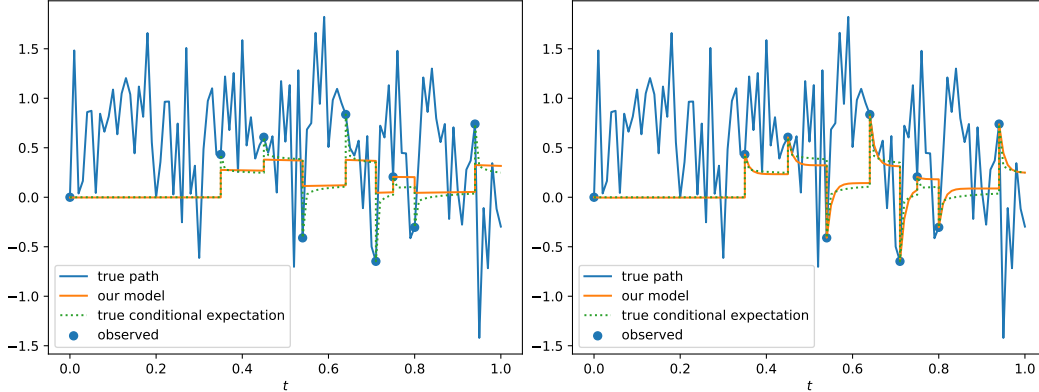


Figure 7: The same test sample of a fractional Brownian motion, when NJ-ODE (with signature) is trained with the original loss function (left) and the equivalent loss function (right). The equivalent loss function prevents NJ-ODE to end up in local minima.

A.2 DETAILS FOR POISSON POINT PROCESS

Dataset. The easiest way to sample of a homogeneous Poisson point process is to use its property that interarrival times are i.i.d. exponential random variables with mean $1/\lambda$. Hence, for each path, we sample as many i.i.d. random variables $E_k \sim Exp(\lambda)$ as needed, such that $\sum_k E_k \geq T$. Then the cumulative sums $(\sum_{k \leq i} E_k)_{i \geq 1}$ are the time points at which the process increases by 1. In between it is constant and its starting point is 0. Finally, the standard discretization time grid is applied to get one sample of the dataset.

Architecture. We use the standard NJ-ODE with the following architecture. The hidden size is $d_H = 10$ and all 3 neural networks have the same structure of 2 hidden layers with tanh activation function and 50 nodes.

A.3 DETAILS FOR UNCERTAINTY ESTIMATION

Architecture. Since the dataset is relatively easy, we test a less complex network here to show that this can already be enough. In particular, we use the standard NJ-ODE with the following architecture. The hidden size is $d_H = 50$, the readout network is a linear map and the other 2 neural networks have the same structure of 1 hidden layer with tanh activation function and 50 nodes.

A.4 DETAILS FOR DEPENDENT OBSERVATION INTENSITY

Architecture. We use the PD-NJ-ODE with the following architecture. The hidden size is $d_H = 50$ and all 3 neural networks have the same structure of 2 hidden layers with tanh activation function and 50 nodes. The signature is used up to truncation level 3.

A.5 DETAILS FOR FRACTIONAL BROWNIAN MOTION

Architecture. We compare the NJ-ODE, the NJ-ODE with signature, the NJ-ODE with recurrent jump network and the PD-NJ-ODE, all with the following architecture. The latent dimension is $d_H = 50$ and all 3 neural networks have the same structure of 2 hidden layers with tanh activation

function and 200 nodes. All truncation levels $m \in \{1, \dots, 10\}$ were tested and level 3 gave the best trade-off between model performance and computation time. Therefore, results are only shown for only for truncation level 3.

A.6 DETAILS FOR CORRELATED 2-DIMENSIONAL BROWNIAN MOTION

Dataset. We use the same methods as described in Appendix A.1.2, but to account for the higher complexity of the dataset, we generate 100'000 samples instead of only 20'000.

Architecture. We use the PD-NJ-ODE with the following architecture. The hidden size is $d_H = 100$, the readout network is a linear map and the other 2 neural networks have the same structure of 1 hidden layer with tanh activation function and 100 nodes. The signature is used up to truncation level 2. This architecture achieves the minimal evaluation metric of $5.2 \cdot 10^{-3}$. When changing to ReLU activation functions, this is nearly halved to $2.8 \cdot 10^{-3}$.

A.7 DETAILS FOR PHYSIONET

Dataset. Details on the dataset are given in (Herrera et al., 2021, Appendix F.5.3). The exact same setup is used.

Architecture. We use the PD-NJ-ODE with the following architecture. The hidden size is $d_H = 50$, and all neural networks have the same structure of 1 hidden layer with tanh activation function and 50 nodes. The signature is used up to truncation level 2. Due to the exponential growth of the network size in the truncation level of the signature, no larger levels were tested.

Training. The training was done as specified in Section A.1.3, except that a batch size of 50 was used for 175 epochs. 5 runs of the same network with random initializations were performed, over which the mean and standard deviation were computed.

Results. The minimal MSE on the test set during the 175 epochs is reported. If instead reporting the MSE of the epoch where the training loss is minimal, the result is $1.957 \pm 0.018 (\times 10^{-3})$, also outperforming the results of NJ-ODE.

A.8 DETAILS FOR LIMIT ORDER BOOK DATASET

Datasets. The widely used benchmark dataset for midprice forecasting (Ntakaris et al., 2018) is unfortunately not suitable in our context, since the time-stamps (or time differences between LOB updates) are not included in the dataset. Hence, the PD-NJ-ODE model could not be applied without adding some artificial time.

Therefore, we test our model on the crypto-currency LOB datasets “BTC”, “BTC1sec” and “ETH1sec” as described in Section 7.7. The datasets have 10'297 (“BTC”), 8'669 (“BTC1sec”) and 8'753 (“ETH1sec”) samples, which are split into the first 80% as training and the last 20% as testing data (such that no lookahead bias is introduced). While the “BTC” is based on the complete LOB of one day (July 2, 2020), the datasets “BTC1sec” and “ETH1sec” are based on snapshots at a frequency of 1 second of roughly 12 days (April 7-19, 2021). The median time step in the “BTC” dataset is approximately 0.025, which means that on average 40 updates of the order book happen every second. However, not every update affects the first 10 levels of the order book in which we are interested. Overall, comparing the number of samples of the datasets, we can conclude that there are roughly 14 updates to the first 10 levels of the order book each second.

The labels (increase, decrease, stationary) for the classification task are computed as outlined in (Zhang et al., 2019, Equation 4), where the threshold α is chosen to be the empirical $\frac{2}{3}$ -quantile of the dataset, such that there is roughly the same number of samples for each label. Importantly, the labels are computed before any other preprocessing is applied to the data, which otherwise might lead to different labels.

For the DeepLOB model, the dataset is normalized by z -scores as it was done in (Zhang et al., 2019). For the PD-NJ-ODE model, the dataset is not normalized, but each sample is shifted such that it starts at $X_0 = 0$ (for the DeepLOB this makes the performance worse, while not shifting for PD-NJ-ODE does not lead to a significant change of the performance). Moreover, the time is shifted such that each sample starts at $t_0 = 0$. Furthermore, we do not use the volume but only the midprice and the bid/ask prices up to level 10 as input for the PD-NJ-ODE.

Architecture. We use the PD-NJ-ODE with the following architecture. The hidden size is $d_H = 100$, and all neural networks have the same structure of 1 hidden layer with tanh activation function and 50 nodes. The signature is used up to truncation level 2, but no recurrent jump network is used. On top of this architecture a classifier network, again with the same structure as the networks above, but with a final softmax activation (to produce outputs in $[0, 1]$ that can be interpreted as probabilities), is used to map the last latent variable H_{t_n} to the class probabilities $(p_{inc}, p_{stat}, p_{dec}) \in [0, 1]^3$. In the additional retraining of the classifier, we also test to use more complex classification networks, which lead to better results. In particular, in the results shown in Table 5, we retrained 3 different classifier networks with the architectures

- 1 hidden layer with tanh activation function and 50 nodes (same as in combined training),
- 2 hidden layers with tanh activation functions and 200 nodes,
- 4 hidden layers with tanh activation functions and 200 nodes,

and reported the results of the best performing one, although all architectures achieved very similar results (less than 3% deviation from reported F1-scores).

Training and Evaluation. The model is first trained for 50 epochs, where the sum (without weighting) of the PD-NJ-ODE loss and the cross-entropy loss of the classifier is minimized with the standard Adam optimizer. The batch size is chosen to be 50 and the learning rate is 0.01. The model is trained to forecast all inputs, i.e., the midprice as well as all bid and ask prices up to level 10, however, in the evaluation of the MSE only the midprice is considered.

The classifier is retrained for 1000 epochs with the cross-entropy loss alone, also with the standard Adam optimizer. The batch size is again 50 and the learning rate is 0.001. For

Training of baseline model DeepLOB. We use the training procedure that was suggested in (Zhang et al., 2019). In particular, the model is trained with a batch size of 64 for 50 epochs and learning rate 0.0001.

Additional Results

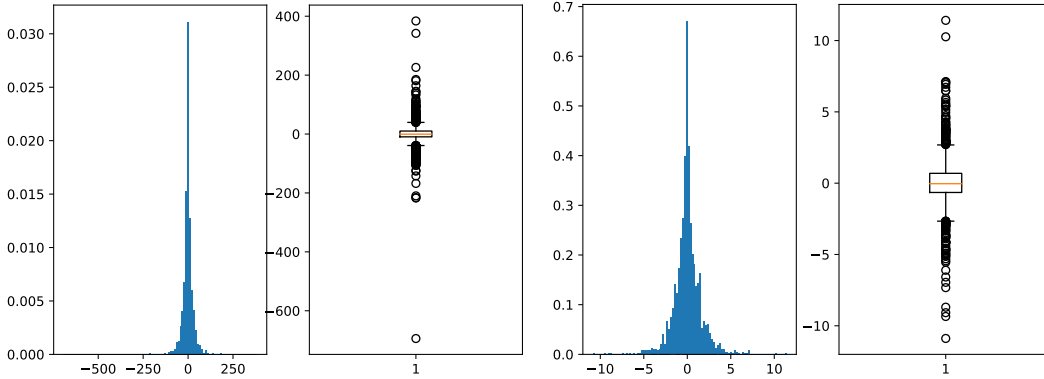


Figure 8: Distribution of the prediction errors of the PD-NJ-ODE model as (density) histogram and boxplot on the BTC1sec (left) and ETH1sec (right) dataset.